医学的に意味のあるものか否かを明確化するためには，種々の疾患患者の血液流動性を測定するとともに，MC-FAN 測定の結果が，生活習慣病の発症や増悪化に関連するかどうかプロスペクティブな調査検討も必要である．

References

1) 菊池佑二：血液をサラサラにする生活術．講談社＋α新書，東京，2001
2) Theilmeier G, Michiels C, Spaepen E, et al : Endothelial von Willebrand factor recruits platelets to atherosclerosis-prone sites in response to hypercholesterolemia. Blood **99**(12) : 4486-4493, 2002
3) Rampling MW : Hyperviscosity as a complication in a variety of disorders. Semin Thromb Hemost **29**(5) : 459-465, 2003
4) Carroll S, Cooke CB, Butterly RJ : Plasma viscosity, fibrinogen and the metabolic syndrome : effect of obesity and cardiorespiratory fitness. Blood Coagul Fibrinolysis **11**(1) : 71-78, 2000
5) Kikuchi, Y : Effect of leukocytes and platelets on blood flow through a parallel array of microchannels : Micro- and macroflow relation and rheological measures of leukocyte and platelet activities. Microvasc Res **50** : 288-300, 1995
6) Colwell JA, Nesto RW : The platelet in diabetes : focus on prevention of ischemic events. Diabetes Care **26**(7) : 2181-2188, 2003
7) Fateh-Moghadam S, Li Z, Ersel S, et al : Platelet degranulation is associated with progression of intima-media thickness of the common carotid artery in patients with diabetes mellitus type 2. Arterioscler Thromb Vasc Biol **25**(6) : 1299-1303, 2005
8) Berndt MC : Induction of platelet-endothelial interactions in postcapillary venules in hypercholesterolemia : critical role of P-selectin. Arterioscler Thromb Vasc Biol **23**(4) : 525-527, 2003
9) Tailor A, Granger DN : Hypercholesterolemia promotes P-selectin-dependent platelet-endothelial cell adhesion in postcapillary venules. Arterioscler Thromb Vasc Biol **23**(4) : 675-680, 2003
10) Kamada H, Hattori K, Hayashi T, et al : In vitro evaluation of blood coagulation activation and microthrombus formation by a microchannel array flow analyzer. Thromb Res **114**(3) : 195-203, 2004

Available online at www.sciencedirect.com
ScienceDirect
Biochemical and Biophysical Research Communications 350 (2006) 598–603
BBRC
www.elsevier.com/locate/ybbrc

Effects of ghrelin and des-acyl ghrelin on neurogenesis of the rat fetal spinal cord

Miho Sato [a], Keiko Nakahara [a], Shintaro Goto [a], Hiroyuki Kaiya [b], Mikiya Miyazato [b], Yukari Date [c], Masamitsu Nakazato [c], Kenji Kangawa [b], Noboru Murakami [a,*]

[a] *Department of Veterinary Physiology, Faculty of Agriculture, University of Miyazaki, Miyazaki 889-2155, Japan*
[b] *National Cardiovascular Center Research Institute, Osaka 565-8565, Japan*
[c] *Third Department of Internal Medicine, University of Miyazaki, Kiyotake, Miyazaki 889-1692, Japan*

Received 6 September 2006
Available online 26 September 2006

Abstract

Expressions of the growth hormone secretagogue receptor (GHS-R) mRNA and its protein were confirmed in rat fetal spinal cord tissues by RT-PCR and immunohistochemistry. *In vitro*, over 3 nM ghrelin and des-acyl ghrelin induced significant proliferation of primary cultured cells from the fetal spinal cord. The proliferating cells were then double-stained using antibodies against the neuronal precursor marker, nestin, and the cell proliferation marker, 5-bromo-2′-deoxyuridine (BrdU), and the nestin-positive cells were also found to be co-stained with antibody against GHS-R. Furthermore, binding studies using [^{125}I]des-acyl ghrelin indicated the presence of a specific binding site for des-acyl ghrelin, and confirmed that the binding was displaced with unlabeled des-acyl ghrelin or ghrelin. These results indicate that ghrelin and des-acyl ghrelin induce proliferation of neuronal precursor cells that is both dependent and independent of GHS-R, suggesting that both ghrelin and des-acyl ghrelin are involved in neurogenesis of the fetal spinal cord.

Keywords: Ghrelin; Des-acyl ghrelin; GHS-R; Neurogenesis; Spinal cord; Fetal development

Ghrelin, a peptide hormone secreted from the stomach, has been identified as the endogenous ligand for the growth hormone secretagogue receptor (GHS-R), through which ghrelin stimulates GH release in the pituitary [1]. Two types of GHS-R, type1a and 1b (GHS-R1a and 1b, respectively), have so far been found, and only the former is able to activate signal transduction of the receptor downstream linking to phospholipase C, resulting in an increase of intracellular calcium [2]. Ghrelin consists of 28 amino acids and is characterized by esterified modification with octanoic acid on serine 3, which is essential for activation of GHSR-1a, although the modification mechanism remains unknown. On the other hand, the level of des-acyl ghrelin, which is inactive on GHS-R1a because of a lack of octanoic acid, is 4 times as high as that of ghrelin in the blood [3].

Many studies have reported that ghrelin has multiple effects other than GH secretion, including regulation of food intake [4] and energy metabolism [5], and gastrointestinal coordination [6,7], as well as facilitation of cell survival, and/or inhibition of apoptosis [8–15]. Although these multiple functions of ghrelin would account for the very wide distribution of GHS-R1a, it is debatable whether GHS-R1a contributes to all of the actions of ghrelin, i.e. that ghrelin may act as a ligand for other types of receptors [16]. So far, however, this possibility remains uninvestigated, and no such alternative receptor has been identified.

We have previously demonstrated that rat fetal growth was increased by treatment of the mother with exogenous ghrelin, and that the effect of ghrelin on fetal growth is diminished by immunization against ghrelin *in vivo* [17]. In addition, we have found that amniotic fluid contains a

* Corresponding author. Fax: +81 985 58 7265.
E-mail address: a0d201u@cc.miyazaki-u.ac.jp (M. Miyazato).

0006-291X/$ - see front matter © 2006 Elsevier Inc. All rights reserved.
doi:10.1016/j.bbrc.2006.09.088

large quantity of des-acyl ghrelin, and that proliferation of cells from rat fetal skin is also stimulated by treatment with both ghrelin and des-acyl ghrelin *in vitro*. On the basis of these findings, we speculate that both ghrelin and des-acyl ghrelin play a crucial role in fetal growth, both peptides acting to facilitate fetal growth not only by enhancement of maternal appetite but also via direct stimulation of fetal cell proliferation by transfer of maternal ghrelin to the fetus.

In the present study, we demonstrated that both ghrelin and des-acyl ghrelin facilitate neural cell proliferation in cultured cells from the fetal spinal cord, which express both the GHS-R gene and its protein, and identified these proliferating cells as neuronal precursor cells. Furthermore, in binding studies using [^{125}I]des-acyl ghrelin, we clarified that des-acyl ghrelin has at least one binding site in the membrane fraction from fetal spinal cord. These results suggest that ghrelin and des-acyl ghrelin can facilitate neurogenesis in the rat fetal spinal cord through both the GHS-R and also an unidentified GHS-R-independent alternative pathway.

Materials and methods

Primary culture of embryonic spinal cord cells. Embryonic spinal cords were obtained from a pregnant rat at day 17. The uterus usually contained 10–14 embryos, 10 of which were utilized for primary culture. The whole spinal cords were mechanically and enzymatically dissociated in papain solution, and the digestion was stopped by addition of culture medium. Cells were passed though a strainer, then centrifuged at 1000 rpm at 4 °C for 10 min and resuspended in DMEM supplemented with $NaHCO_3$, antibiotics (penicillin, streptomycin; Sigma, MO), and 5% fetal calf serum, followed by plating onto laminin-coated 96-well plates at 10^5 cells per well.

Ghrelin and des-acyl ghrelin treatment and cell proliferation assay. Cell proliferation was measured by Cell Proliferation ELISA with BrdU (Roche Diagnostic GmbH, Mannheim, Germany) according to the manufacturer's instructions with some optimization for the present cell conditions as follows. Briefly, after incubation for four days, the cells were treated with ghrelin or des-acyl ghrelin at a final concentration of 0.003–300 nM for 12 h. Subsequently, BrdU was added to the cells to label newly synthesized DNA, followed by further incubation for 6 h. After incubation, the cells were fixed and denatured, and incubated with anti-BrdU antibody for 90 min. Each well was washed out and reacted with substrate solution until color development. The absorbance of the reaction was measured by an immunoreader. Data were expressed as means ± SEM. The significance of differences between the control and treated cells was analyzed by Student's t test. Differences at $P < 0.05$ were considered statistically significant.

Immunohistochemistry. Frozen sections of the embryonic spinal cord 14 μm thick were prepared from embryos at embryonic day (ED) 17 and fixed with 4% paraformaldehyde in 0.1 M phosphate buffer for 30 min. After washing with 0.1 M phosphate buffer, the preparations were incubated with 2% normal goat serum in PBS for 30 min at room temperature, washed with PBS three times, and incubated overnight at 4 °C with each of the following primary antibodies: Polyclonal rabbit anti-microtubule-associated protein 2 (Map2; 1:1000, Chemicon International, Inc., CA), anti-neurofilament H (NF-H; 1:1000, Chemicon International), and anti-GHS-R and monoclonal mouse anti-nestin (1:10,000, Chemicon International). Subsequently, all the sections were washed in PBS and incubated with Alexa Fluor 488-conjugated goat anti-rabbit IgG, except the sections that were incubated with the anti-nestin antibody, for which FITC-conjugated goat anti-mouse IgG (1:200, Chemicon International) was used as the secondary antibody. After washing out the residual antibodies and embedding of the sections, they were observed using a light microscope.

Cultured spinal cord cells, which had incorporated BrdU after incubation for 4 days during the ELISA preparation procedure, were fixed with methanol and glacial acetic acid at −20 °C for 20 min. After DNA denaturation with 2 M HCl and blocking with 2% normal goat serum in PBS for 30 min at room temperature, the fixed cells were incubated overnight at 4 °C with either anti-Map2 or anti-nestin as the primary antibody. Afterwards, the cells were incubated at RT for 1 h with the same secondary antibodies as those used for staining the frozen sections. After the washing step, the cells were further incubated with rat anti-BrdU monoclonal antibody (1:1000, Abcam, Cambridge, UK) as a primary antibody for double staining, followed by incubation with Cy^{TM}3-conjugated donkey anti-rat IgG polyclonal antibody (1:1000, Jackson Immuno Research Laboratories, Inc., PA) as the secondary antibody. For double staining of the GHS-R for either Map2 or nestin, cells fixed with 4% paraformaldehyde in 0.1 M phosphate buffer were first incubated with either mouse anti-Map2 or anti-nestin primary antibody, and then with rabbit anti-GHS-R antibody.

RT-PCR. Total RNA was isolated from the spinal cord of embryos at ED 13, 15, 17, 19, and postnatal day (PD) 0 using Trizol Reagent (Life Technologies, Inc., Gaithersburg, MD). Single-strand DNA was generated from 1 μg of total RNA with the use of Superscript 3 preamplification reagent (Life Technologies, Inc., Bethesda, MD) according to the manufacturer's instructions. PCR was carried out using a BD advantage^{TM} 2 PCR Enzyme System (BD Science, CA). The PCR primers specific for GHS-R1a were 5′-GATACCTCTTTTCCAAGTCCTTCGAGCC-3′ for sense and 5′-TTGAACACTGCCACCCGGTACTTCT-3′ for antisense (nucleotides 842–869 and 1001–1025; Accession No. AB001982, GenBank), and those specific for GAPDH were 5′-CGGCAAGTTCA ACGGCACA-3′ for sense and 5′-AGACGCCAGTAGACTCCACGA CA-3′ for antisense (nucleotides 1002–1020 and 1125–1147; Accession No. AF106860, GenBank).

Des-acyl ghrelin binding assay. Binding of des-acyl ghrelin to tissue membranes of fetal spinal cord was studied using [^{125}I]des-acyl ghrelin as a radioligand. Membrane fractions (30,000g pellet) were isolated from fetal spinal cord tissue as described previously [18–20]. Membranes with a protein content of 10 μg, as determined by the Lowry method, were incubated at 4 °C for 1 h with increasing concentrations (0.13–16.64 nM) of [^{125}I]des-acyl ghrelin in a final volume of 0.5 ml assay buffer (50 mM Tris–HCl, 2.5 mM EGTA, 0.1% BSA, and protease inhibitor cocktail (Sigma, MO), pH 7.4). Parallel incubations in the presence of 1.0 μM unlabeled des-acyl ghrelin were used to determine nonspecific binding, which was subtracted from total binding to yield specific binding values. For competition assay, tissue membranes were incubated with 0.1 nM labeled des-acyl ghrelin and either unlabeled des-acyl ghrelin or ghrelin at 4 °C for 1 h. After incubation, the reaction solution was filtered through Whatman GF/B filters, which were then rinsed three times with assay buffer. The radioactivity of the membranes on the filter was measured with a gamma counter. Saturation isotherms were transformed using the method of Scatchard and the maximal number of binding sites (B_{max}) and the dissociation constant (K_d) were calculated using the GraphPAD Prism 4 program (GraphPAD Software, CA).

Results

GHS-R mRNA and protein expression in fetal spinal cord

Using RT-PCR, we examined GHS-R mRNA expression in spinal cords obtained from rat fetuses at ED 13, 15, 17, 19, and PD 0 (Fig. 1a). Abundant levels of GHS-R mRNA were expressed in the spinal cord in fetuses at all ages examined, as we have reported previously [17]. We then investigated GHS-R expression at the protein level by immunohistochemistry. At the same time, we detected neuronal cells by using antibodies against the neuron-specific markers Map2 and NF-H, as well as nestin for

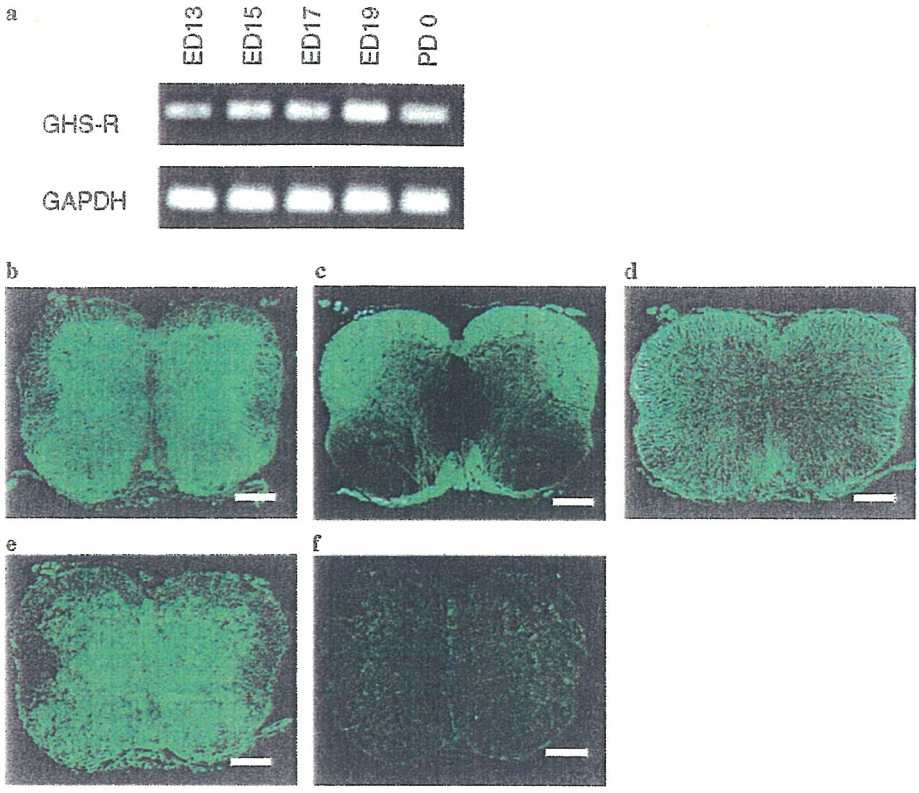

Fig. 1. (a) Detection of GHS-R mRNA in the rat fetal spinal cord by RT-PCR. The PCR product amplified with primers specific for GHS-R1a was detected from embryonic day (ED) 13 to postnatal day (PD) 0. GAPDH mRNA was also detected as an internal control. (b–f) Immunofluorescence staining with antibodies against neuron marker and GHS-R proteins in the rat fetal spinal cord. Map2-positive (b) and Neurofilament H-positive cells (c) were localized in the gray and white matters, respectively. Immunoreactivity of the neuronal precursor cell marker, nestin, was found throughout the spinal cord but with strongest staining in the white matter (d) GHS-R immunoreactivity was localized in the gray matter (e) and was not observed in sections that had been exposed to the preadsorbing antibody (f). Bars, 200 μm.

neuroprogenitor cells. Cells immunoreactive for Map2 were located in the core of the spinal cord, the so-called gray matter (Fig. 1b), while NF-H immunoreactivity was confirmed in the white matter (Fig. 1c). Nestin-positive cells were located in all regions, but the most intense staining was observed in the white matter (Fig. 1d). GHS-R-positive staining was located in the gray matter of the spinal cord (Fig. 1e), and the staining was abolished by pre-absorption of the antibody (Fig. 1f).

Proliferation of spinal cord cells upon treatment with ghrelin and des-acyl ghrelin

Primary culture of spinal cord cells from rat fetus at ED17 was performed. The cells were cultured with BrdU for 6 h after initial incubation for 4 days, and then treated with ghrelin and des-acyl ghrelin for a further 12 h. BrdU is incorporated into DNA when cells synthesize DNA during the S phase of the cell cycle and can be immunodetected using anti-BrdU antibody. BrdU-positive cells were detected under all conditions, irrespective of treatment, although BrdU positivity was more abundant in cells that had been cultured with ghrelin and des-acyl ghrelin than in non-treated cells. To quantify the increase in the number of cells positive for BrdU, we measured cell proliferation by BrdU ELISA. Treatment with both ghrelin (Fig. 2a) and des-acyl ghrelin (Fig. 2b) at over 3 nM significantly increased the incorporation of BrdU.

Identification of the proliferative cell type and cell type expressing GHS-R

Immunofluorescence double staining of cultured cells treated with ghrelin that had incorporated BrdU into their DNA was performed to identify proliferating cells among cultured rat fetal spinal cord cells. Cells with Map2 positivity showed a typical neuron-like shape with extended dendrites and did not show BrdU positivity in their nuclei (Fig. 3a). Cells with nestin positivity were pleomorphic and showed BrdU positivity in their nuclei, i.e., neuronal precursor cells (Fig. 3b). In addition, BrdU positivity was also found in cells that were unstained by antibodies against both Map2 and nestin (data not shown). GHS-R-expressing cells were then examined by immunofluorescence double staining, as was the case for cultured cells without BrdU treatment. GHS-R immunoreactivity was observed in the nestin-positive cells (Fig. 3c).

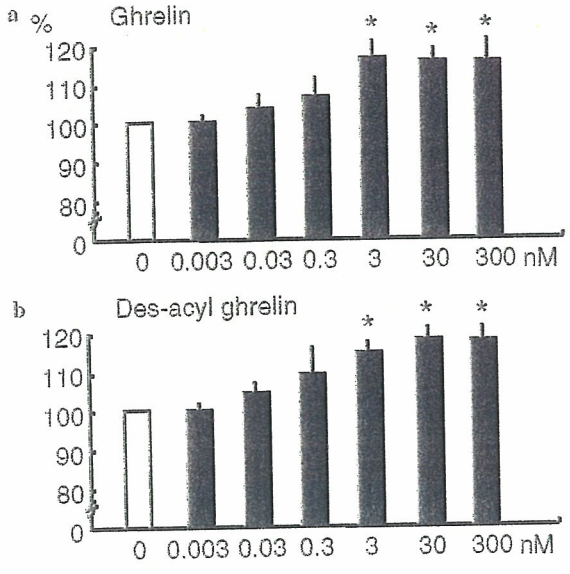

Fig. 2. Cell proliferation effects of ghrelin and des-acyl ghrelin on cultured fetal spinal cells. Proliferative cells were quantified by BrdU ELISA. Significant proliferation was indicated in cells treated with over 3 nM ghrelin (a) and des-acyl ghrelin (b). Values are presented by means ± SEM ($^*P < 0.05$).

Binding assay

To identify the presence of the binding site of des-acyl ghrelin, [^{125}I]des-acyl ghrelin binding to membranes from fetal spinal cord was assayed. Specific, high affinity and saturable binding of labeled ghrelin were observed ($K_d = 3.467$, $B_{max} = 1.061$ fmol/mg protein) (Fig. 4a). The binding of labeled des-acyl ghrelin was displaced by unlabeled des-acyl ghrelin and ghrelin (Fig. 4b). The IC_{50} values for des-acyl ghrelin and ghrelin were 23.52 and 41.60 nM, respectively.

Discussion

Our previous study showed that ghrelin, as well as des-acyl ghrelin, play important roles in fetal growth, and that GHS-R mRNA is abundantly expressed in the spinal cord of rat fetus compared with other tissues [17]. Therefore, we reasoned that these ligands and their receptor might exert important actions during neurogenesis of the embryonic spinal cord. In the present study, in fact, ghrelin and des-acyl ghrelin both facilitated the proliferation of cells from fetal spinal cord. In addition, GHS-R mRNA and

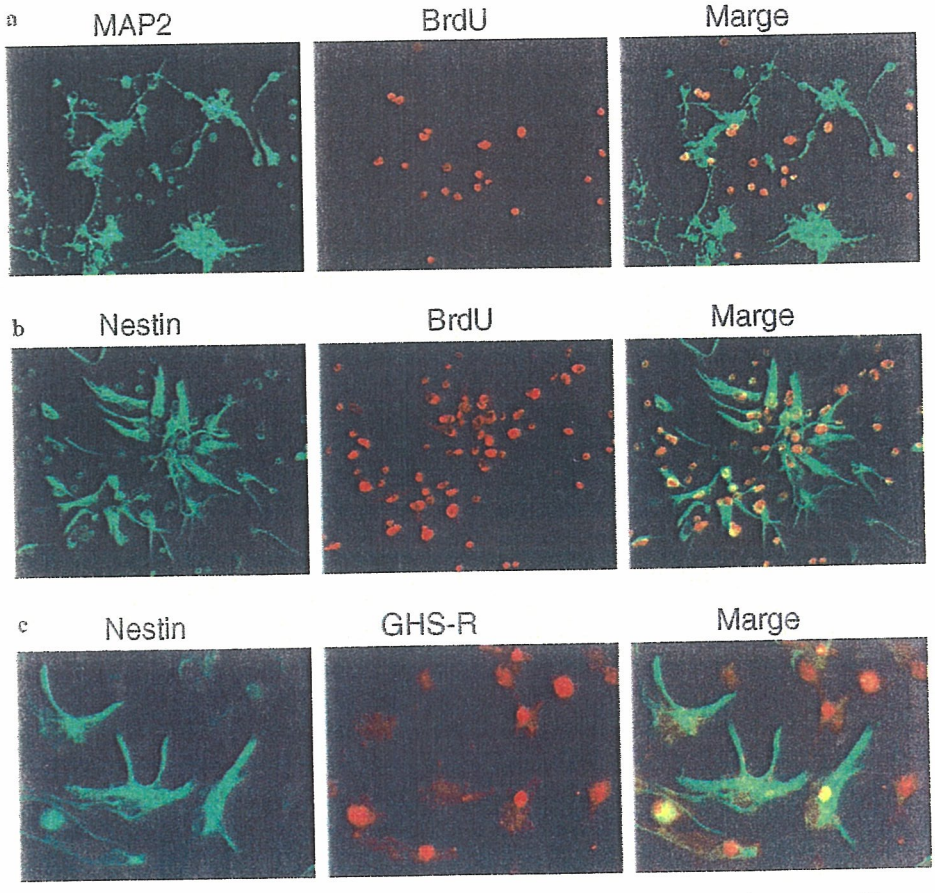

Fig. 3. Identification of proliferative cells in the rat fetal spinal cord. Double immunofluorescence staining demonstrated immunoreactivity for both Map2 and BrdU in distinct cells (a), and co-localization of nestin and BrdU in the same cells (b) Co-localization of nestin and GHS-R was also observed in neuron precursor cells (c).

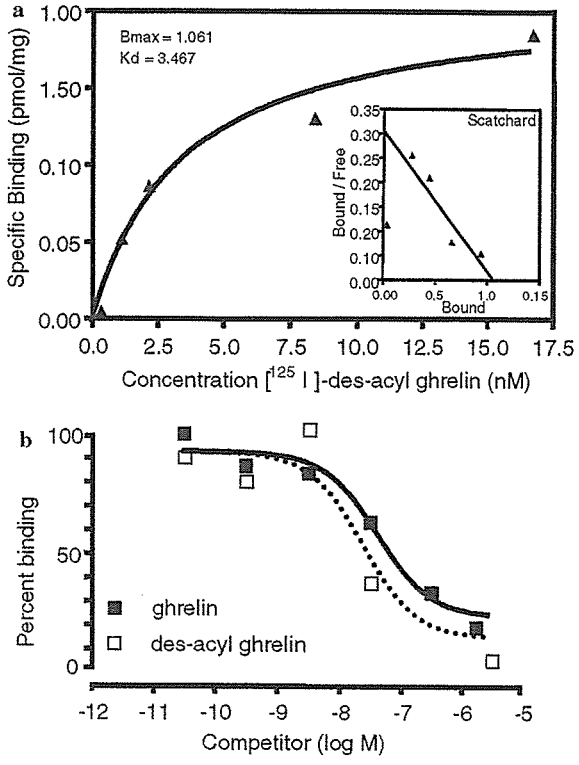

Fig. 4. (a) Representative saturation curve and the Scatchard plot of [^{125}I]des-acyl ghrelin binding to membranes from the fetal spinal cord. Binding assay was performed by incubating a fixed amount of membranes with increasing concentrations (0.13–16.64 nM) of the radioligand. Specific binding values were obtained by subtracting non-specific binding from total binding. (b) Displacement curve of [^{125}I]des-acyl ghrelin binding in the presence of unlabeled des-acyl ghrelin or ghrelin. Binding assay was performed by incubation of fixed amounts of membranes and labeled ligand with increasing concentrations of either of the unlabeled ligands.

GHS-R protein were detected in spinal cord tissue, and neuronal precursor cells in primary culture possessed GHS-R immunoreactivity, indicating that ghrelin stimulated the proliferation of neuronal precursor cells through GHS-R. Although the receptor recognizing des-acyl ghrelin has not yet been characterized, the present binding study indicated that there was at least one binding site specific for des-acyl ghrelin in membranes from fetal spinal cord tissue. Several recent studies have reported that not only ghrelin but also des-acyl ghrelin exert a biological effect even in tissues or cells that do not express GHS-R, suggesting that these reactions would not require octanoic acid modification and could be achieved without GHS-R [11,17,21,22]. Interestingly, many of the effects induced by both peptides at the cellular level are associated with cell fate, such as cell survival and/or apoptosis as well as cell proliferation, although activation or inhibition of the cell survival and proliferation pathways appear to be independent of cell type [11]. Thus, it is assumed that the effect of ghrelin and des-acyl ghrelin on spinal cord cells observed in the present study could be induced through both the GHS-R and another unknown pathway.

Recently, Zhang et al. demonstrated that ghrelin acted directly on dorsal motor nucleus of the vagus neurons to stimulate neurogenesis, and concluded that neuronal proliferation would result from an increase of calcium concentration associated with cellular depolarization through activation of GHSR-1a by ghrelin [15]. In the present study, however, diltiazem, a blocker of L-type voltage-dependent calcium channels, did not inhibit proliferation of spinal cord neuronal cells, inconsistent with dorsal motor nucleus of the vagus neurons, suggesting that the proliferation effect was likely mediated via a pathway other than the calcium increase caused by depolarization of L-type calcium channels (data not shown). Some studies of the molecular mechanism involved in the induction of cell proliferation and adhesion by ghrelin have suggested cascades of intracellular events, such as the MAPK and/or PI3 K/Akt pathways. In hepatoma cells expressing GHS-R, ghrelin has been shown to activate the IRS-1-GRB2-MAPK pathway, downstream from the insulin receptor, but to inhibit Akt activity [23]. Also in cardiomyocytes and endothelial cells, ghrelin induces phosphorylation of tyrosine, and both ghrelin and des-acyl ghrelin activate the MAPK and Akt pathways [9]. In addition, activation of the MAPK pathway by ghrelin has also been reported in a rat pituitary somatotroph cell line [13] and human adrenal zona glomerulosa cells [12]. Nanzer has explained the possible pathways leading to MAPK activation, resulting from stimulation of phospholipase C and PKC, or transactivation of tyrosine kinase receptors via the beta and gamma subunits of the G protein. Similarly, it is assumed that the cell proliferation effect of ghrelin and des-acyl ghrelin in the rat fetal spinal cord might involve activation of MAPK and/or PI3K/AKt.

In this study, not only neuronal precursor cells but also neurons seemed to possess GHS-R protein, because the localization of Map-2-positive cells was consistent with that of GHS-R-positive cells in sections of spinal cord tissue. These results suggested that ghrelin would play an unidentified role via GHS-R in neurons of the rat fetus, for instance during formation of the neuronal network. Although there is no evidence of any abnormality in GHS-R-knockout mouse fetus [24], this function as well as the cell proliferative effect may be concealed by compensating actions of growth factors such as nerve growth factor.

In summary, we have demonstrated that both the GHS-R gene and protein are expressed in the rat fetal spinal cord from ED 13 to PD 0. In primary cultures of fetal spinal cord cells, ghrelin and des-acyl ghrelin induced cell proliferation effects, whereby neuronal precursor cells possessing GHS-R protein were increased. Moreover, a binding study using labeled des-acyl ghrelin showed that specific binding to des-acyl ghrelin could be displaced by unlabeled ghrelin and des-acyl ghrelin in membranes from fetal spinal cord. Taken together, our findings suggest that in the rat fetal spinal cord, ghrelin and des-acyl ghrelin are involved in neurogenesis via both GHS-R and an unidentified receptor

for des-acyl ghrelin. Further examinations to identify this unknown receptor for des-acyl ghrelin are warranted.

Acknowledgments

This study was supported in part by the Program for Promotion of Basic Research Activities for Innovative Bioscience (PROBRAIN), the Mitsubishi Foundation, and a Grant-in-Aid for the Promotion of Evolutional Science and Technology in Miyazaki Prefecture (NM).

References

[1] M. Kojima, H. Hosoda, Y. Date, M. Nakazato, H. Matsuo, K. Kangawa, Ghrelin is a growth-hormone-releasing acylated peptide from stomach, Nature 402 (1999) 656–660.

[2] A.D. Howard, S.D. Feighnerm, D.F. Cully, J.P. Arena, P.A. Liberator, C.I. Rosenblum, M. Hamelin, D.L. Hreniuk, O.C. Palyha, J. Anderson, P.S. Paress, C. Diaz, M. Chou, K.K. Liu, K.K. McKee, S.S. Pong, L.Y. Chaung, A. Elbrecht, M. Dashkevicz, R. Heavens, M. Rigby, D.J. Sirinathsinghji, D.C. Dean, D.G. Mellilo, A.A. Patchett, R. Nargund, R.G. Patrick, J.A. DeMartino, S.K. Gupta, J.M. Shaeffer, R.G. Smith, L.H. Van der Ploeg, A receptor in pituitary and hypothalamus that functions in growth hormone release, Science 273 (1996) 974–977.

[3] H. Hosoda, M. Kojima, H. Matsuo, K. Kangawa, Ghrelin and des-acyl ghrelin: two major forms of rat ghrelin peptide in gastrointestinal tissue, Biochem. Biophys. Res. Commun. 279 (2000) 909–913.

[4] M. Nakazato, N. Murakami, Y. Date, M. Kojima, H. Matsuo, K. Kangawa, S. Matsukura, A role for ghrelin in the central regulation of feeding, Nature 409 (2001) 194–198.

[5] M. Tschop, D.L. Smiley, M.L. Heiman, Ghrelin induces adiposity in rodents, Nature 407 (2000) 908–913.

[6] Y. Masuda, T. Tanaka, N. Inomata, N. Ohnuma, S. Tanaka, Z. Itoh, H. Hosoda, M. Kojima, K. Kangawa, Ghrelin stimulates gastric acid secretion and motility in rats, Biochem. Biophys. Res. Commun. 276 (2000) 905–908.

[7] Y. Date, M. Nakazato, N. Murakami, M. Kojima, K. Kangawa, S. Matsukura, Ghrelin acts in the central nervous system to stimulate gastric acid secretion, Biochem. Biophys. Res. Commun. 280 (2001) 904–907.

[8] I. Pettersson, G. Muccioli, R. Granata, R. Deghenghi, E. Ghigo, C. Ohlsson, Natural (ghrelin) and synthetic (hexarelin) GH secretagogues stimulate H9c2 cardiomyocyte cell proliferation, J. Endocrinol. 175 (2002) 201–209.

[9] G. Baldanzi, N. Filigheddu, S. Cutrupi, F. Catapano, S. Bonissoni, A. Fubini, D. Malan, G. Baj, R. Granata, F. Broglio, M. Papotti, N. Surico, F. Bussolino, J. Isgaard, R. Deghenghi, F. Sinigaglia, M. Prat, G. Muccioli, E. Ghigo, A. Graziani, Ghrelin and des-acyl ghrelin inhibit cell death in cardiomyocytes and endothelial cells through ERK1/2 and PI 3-kinase/AKT, J. Cell. Biol. 159 (2002) 1029–1037.

[10] M.S. Duxbury, T. Waseem, H. Ito, M.K. Robinson, M.J. Zinner, S.W. Ashley, E.E. Whang, Ghrelin promotes pancreatic adenocarcinoma cellular proliferation and invasiveness, Biochem. Biophys. Res. Commun. 309 (2003) 464–468.

[11] P. Cassoni, C. Ghe, T. Marrocco, E. Tarabra, E. Allia, F. Catapano, R. Deghenghi, E. Ghigo, M. Papotti, G. Muccioli, Expression of ghrelin and biological activity of specific receptors for ghrelin and des-acyl ghrelin in human prostate neoplasms and related cell lines, Eur. J. Endocrinol. 150 (2004) 173–184.

[12] G. Mazzocchi, G. Neri, M. Rucinski, P. Rebuffat, R. Spinazzi, L.K. Malendowicz, G.G. Nussdorfer, Ghrelin enhances the growth of cultured human adrenal zona glomerulosa cells by exerting MAPK-mediated proliferogenic and antiapoptotic effects, Peptides 25 (2004) 1269–1277.

[13] A.M. Nanzer, S. Khalaf, A.M. Mozid, R.C. Fowkes, M.V. Patel, J.M. Burrin, A.B. Grossman, M. Korbonits, Ghrelin exerts a proliferative effect on a rat pituitary somatotroph cell line via the mitogen-activated protein kinase, Eur. J. Endocrinol. 151 (2004) 233–240.

[14] M.S. Kim, C.Y. Yoon, P.G. Jang, Y.J. Park, C.S. Shin, H.S. Park, J.W. Ryu, Y.K. Pak, J.Y. Park, K.U. Lee, S.Y. Kim, H.K. Lee, Y.B. Kim, K.S. Park, The mitogenic and antiapoptotic actions of ghrelin in 3T3-L1 adipocytes, Mol. Endocrinol. 18 (2004) 2291–2301.

[15] W. Zhang, T.R. Lin, Y. Hu, Y. Fan, L. Zhao, E.L. Stuenkel, M.W. Mulholland, Ghrelin stimulates neurogenesis in the dorsal motor nucleus of the vagus, J. Physiol. 559 (2004) 729–737.

[16] E. Ghigo, F. Broglio, E. Arvat, M. Maccario, M. Papotti, G. Muccioli, Ghrelin: more than a natural GH secretagogue and/or an orexigenic factor, Clin. Endocrinol. 62 (2005) 1–17.

[17] K. Nakahara, M. Nakagawa, Y. Baba, M. Sato, K. Toshinai, Y. Date, M. Nakazato, M. Kojima, M. Miyazato, H. Kaiya, H. Hosoda, K. Kangawa, N. Murakami, Maternal ghrelin plays an important role in fetal development during pregnancy, Endocrinol. 147 (2006) 1333–1342.

[18] G. Muccioli, C. Ghe, M.C. Ghigo, M. Papotti, E. Arvat, M.F. Boghen, M.H. Nilsson, R. Deghenghi, H. Ong, E. Ghigo, Specific receptors for synthetic GH secretagogues in the human brain and pituitary gland, J. Endocrinol. 157 (1998) 99–106.

[19] I. Bedendi, G. Alloatti, A. Marcantoni, D. Malan, F. Catapano, C. Ghe, R. Deghenghi, E. Ghigo, G. Muccioli, Cardiac effects of ghrelin and its endogenous derivatives des-octanoyl ghrelin and des-Gln14-ghrelin, Eur. J. Pharmacol. 476 (2003) 87–95.

[20] G. Muccioli, N. Pons, C. Ghe, F. Catapano, R. Granata, E. Ghigo, Ghrelin and des-acyl ghrelin both inhibit isoproterenol-induced lipolysis in rat adipocytes via a non-type 1a growth hormone secretagogue receptor, Eur. J. Pharmacol. 498 (2004) 27–35.

[21] C.Y. Chen, A. Inui, A. Asakawa, K. Fujino, I. Kato, C.C. Chen, N. Ueno, M. Fujimiya, Des-acyl ghrelin acts by CRF type 2 receptors to disrupt fasted stomach motility in conscious rats, Gastroenterol. 129 (2005) 8–25.

[22] C. Gauna, P.J. Delhanty, L.J. Hofland, J.A. Janssen, F. Broqlio, R.J. Ross, E. Ghiqo, A.J. van der Lelv, Ghrelin stimulates, whereas des-octanoyl ghrelin inhibits, glucose output by primary hepatocytes, J. Clin. Endocrinol. Metab. 90 (2005) 1055–1060.

[23] M. Murata, Y. Okimura, K. Iida, M. Matsumoto, H. Sowa, H. Kaji, M. Kojima, K. Kangawa, K. Chihara, Ghrelin modulates the downstream molecules of insulin signaling in hepatoma cells, J. Biol. Chem. 277 (2002) 5667–5674.

[24] Y. Sun, P. Wang, H. Zheng, R.G. Smith, Ghrelin stimulation of growth hormone release and appetite is mediated through the growth hormone secretagogue receptor, Proc. Natl. Acad. Sci. USA 101 (2004) 4679–4684.

Peripheral ghrelin transmits orexigenic signals through the noradrenergic pathway from the hindbrain to the hypothalamus

Yukari Date,[1,8,*] Takuya Shimbara,[1,8] Shuichi Koda,[1,3] Koji Toshinai,[1] Takanori Ida,[4] Noboru Murakami,[4] Mikiya Miyazato,[5] Koichi Kokame,[6] Yuta Ishizuka,[2] Yasushi Ishida,[2] Haruaki Kageyama,[7] Seiji Shioda,[7] Kenji Kangawa,[5] and Masamitsu Nakazato[1]

[1] Third Department of Internal Medicine
[2] Department of Psychiatry
Miyazaki Medical College, University of Miyazaki, Miyazaki 889-1692, Japan
[3] Biomedical Research Laboratories, Daiichi Asubio Pharma Co., Ltd., Osaka 681-8513, Japan
[4] Department of Veterinary Physiology, Faculty of Agriculture, Miyazaki University, Miyazaki 889-2192, Japan
[5] Department of Biochemistry
[6] Department of Vascular Physiology
National Cardiovascular Center Research Institute, Osaka 565-8565, Japan
[7] Department of Anatomy, Showa University School of Medicine, Tokyo142-8555, Japan
[8] These authors contributed equally to this work.
*Correspondence: dateyuka@med.miyazaki-u.ac.jp

Summary

Ghrelin, a gastrointestinal peptide, stimulates feeding when administered peripherally. Blockade of the vagal afferent pathway abolishes ghrelin-induced feeding, indicating that the vagal afferent pathway may be a route conveying orexigenic ghrelin signals to the brain. Here, we demonstrate that peripheral ghrelin signaling, which travels to the nucleus tractus solitarius (NTS) at least in part via the vagus nerve, increases noradrenaline (NA) in the arcuate nucleus of the hypothalamus, thereby stimulating feeding at least partially through α-$_1$ and β-$_2$ noradrenergic receptors. In addition, bilateral midbrain transections rostral to the NTS, or toxin-induced loss of neurons in the hindbrain that express dopamine β hydroxylase (an NA synthetic enzyme), abolished ghrelin-induced feeding. These findings provide new evidence that the noradrenergic system is necessary in the central control of feeding behavior by peripherally administered ghrelin.

Introduction

Ghrelin, a newly discovered member of the family of gut-brain peptides, functions in feeding control and growth hormone (GH) secretion by binding to the growth hormone secretagogue receptor (GHS-R) (Kojima et al., 1999; Nakazato et al., 2001; Tschöp et al., 2000; Wren et al., 2000). This peptide, which is produced primarily by endocrine cells of the stomach, is released into the circulation (Date et al., 2000; Dornonville de la Cour et al., 2001). Ghrelin is also produced by neurons of the hypothalamus, where it serves as part of the neural networks (Cowley et al., 2003). GHS-R is extensively distributed throughout the brain, including the hypothalamus and brainstem where are essential for energy homeostasis. Given the GHS-R expression pattern, ghrelin, when given centrally, peripherally, or both, may increase food intake directly via effects on neurons present in the hypothalamus or brainstem. We recently demonstrated, however, that blockade of the gastric vagal afferent pathway abolished peripheral ghrelin-induced feeding (Date et al., 2002). A similar study demonstrated that intraperitoneal injection of ghrelin into vagotomized mice did not stimulate food intake (Asakawa et al., 2001). These findings suggest that the gastric vagal afferent pathway as well as the humoral pathway may have some significant part in conveying ghrelin-mediated orexigenic signals to the brain.

Several gastrointestinal hormones, including ghrelin, cholecystokinin (CCK), peptide YY, and glucagon-like peptide 1, transmit signals of starvation and satiety to the brain at least in part via the vagal afferent system (Date et al., 2002; Smith et al., 1981; Koda et al., 2005; Abbott et al., 2005). Feeding-related information, travels directly to the nucleus tractus solitarius (NTS), where it can be converted to additional signals that transmit a feeling of hunger or fullness to the hypothalamus. In the present study, we focused on the importance of the neural pathways from the NTS to the hypothalamus in transmitting peripheral ghrelin signals.

To investigate the neural pathways involved in the transmission of ghrelin orexigenic signals from the NTS to the hypothalamus, we examined the effects of bilateral midbrain transections on ghrelin-induced feeding. The NTS contains the A2 noradrenergic cell group, which projects to regions of the hypothalamus that include the arcuate nucleus (ARC) (Sawchenko and Swanson, 1981). Therefore, we examined the role of the central noradrenaline (NA) system in peripheral ghrelin feeding stimulation. Using real-time PCRs, we quantified the expression of dopamine β hydroxylase (DBH), an enzyme necessary to convert dopamine into NA, within the NTS. We also measured overflow NA within or near the ARC after intravenous administration of ghrelin using in vivo microdialysis. We studied the effects of adrenergic antagonists and the elimination of NA innervation within the ARC on ghrelin-induced food intake. Using immunohistochemical techniques, we demonstrated that the NPY neurons activated following intravenous administration of ghrelin are innervated by DBH-containing fibers.

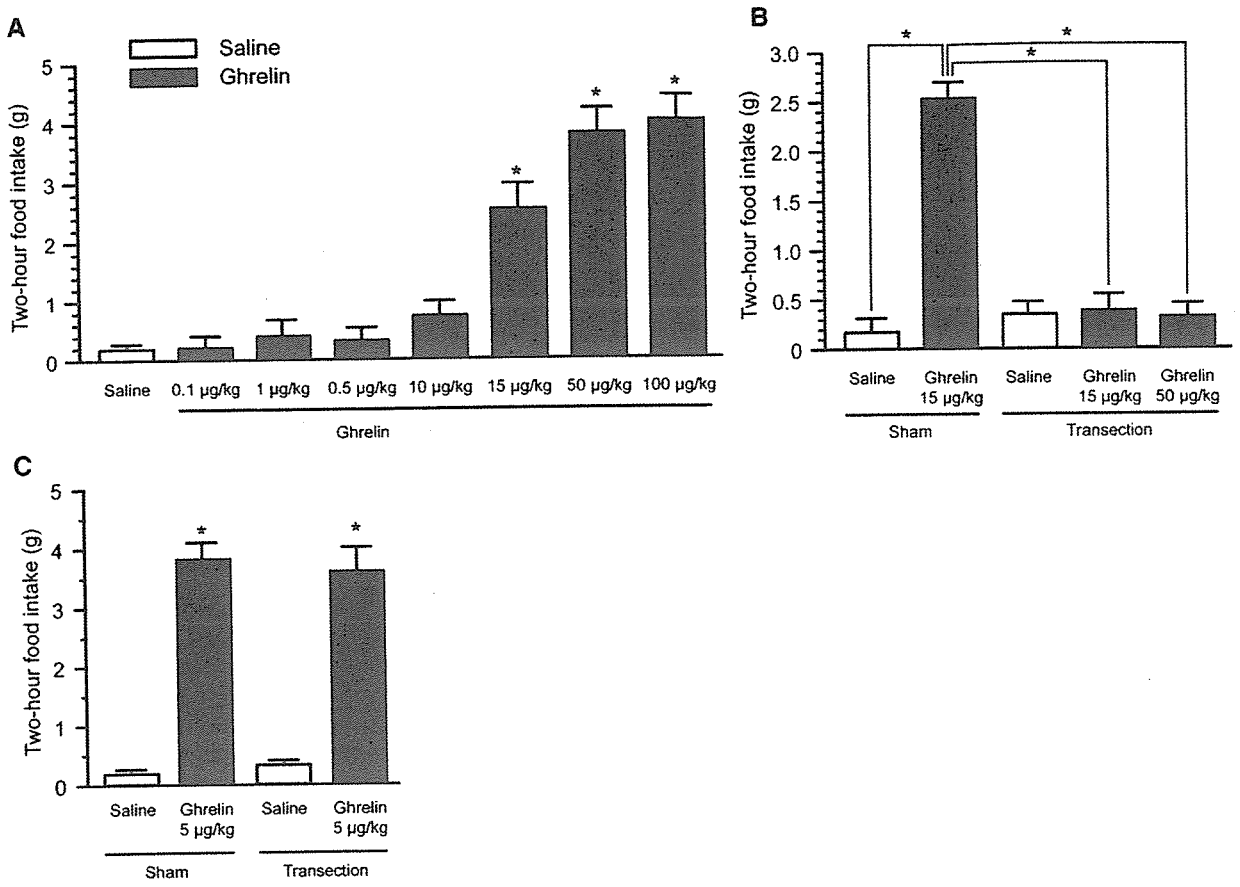

Figure 1. Effect of bilateral midbrain transections on ghrelin-induced feeding behavior

A) Two hour food intake (mean ± SEM) of sham-treated rats after a single intravenous administration of ghrelin (0.1–100 μg/kg). *$p < 0.0001$ versus saline.

B) Food intake of rats with bilateral midbrain transections after a single intravenous administration of ghrelin (15 and 50 μg/kg). *$p < 0.0001$.

C) Food intake of rats with bilateral midbrain transections after single intracerebroventricular administration of ghrelin (5 μg/kg). *$p < 0.0001$.

Error bars represent the SEM.

Results and Discussion

Midbrain transections and peripheral ghrelin-induced feeding

To investigate if intravenous administration of ghrelin stimulates feeding via the ascending efferent fibers of the NTS, we examined ghrelin-induced food intake in rats with bilateral midbrain transections (Crawley et al. 1984). Before this experiment, we confirmed that there were no significant differences in body weight or food intake between control and actual transected groups up to eight days after the surgery (see Supplemental Results and Figure S1 in the Supplemental Data available with this article online). There were also no significant differences in the feeding response after fasting for 12 hr, energy expenditure, locomotor activity, body fat, or food preference between the two groups seven days after surgery (Supplemental Results and Figure S2). Therefore, we performed feeding experiments using rats seven days after the surgery. The lowest effective dose of intravenously (i.v.) administered ghrelin for rats subjected to sham surgery (sham-treated rats) was 15 μg/kg; this value was used as the standard dose in the subsequent experiments (Figure 1A). Intravenous administration of ghrelin (≥ 15 μg/kg) significantly increased food intake (10:00–12:00 hr) in sham-treated rats, whereas ghrelin-induced feeding was absent in midbrain transected rats (Figure 1B) (n = 10 per group). Because bilateral midbrain transections may nonspecifically suppress feeding in response to ghrelin, we tested the orexigenic effect of centrally administered ghrelin in the midbrain transected rats. Intracerebroventricular administration of ghrelin similarly increased food intake in the transected and control groups (Figure 1C) (n = 7 per group). This finding demonstrates that bilateral midbrain transections specifically blocked peripherally administered ghrelin-induced feeding, but did not affect centrally administered ghrelin-induced feeding. Centrally and peripherally administered ghrelin may therefore stimulate feeding by distinct mechanisms. Midbrain transections severing the ascending efferent fibers of the NTS block feeding reduction of CCK that transmits satiety signals to the brain via the afferent limb of the vagus nerve (Crawley et al., 1984). In contrast, Grill and Smith showed that CCK-induced feeding reduction is still observed in chronic decerebrate rats (Grill and Smith, 1988). We described some differences in the surgery between midbrain transection and chronic decerebration in Supplementary Methods (Grill and Norgren, 1978) (Supplemental Experimental Procedures).

We have already shown the possibility that peripheral ghrelin signals for starvation are transmitted to the neuropeptide Y

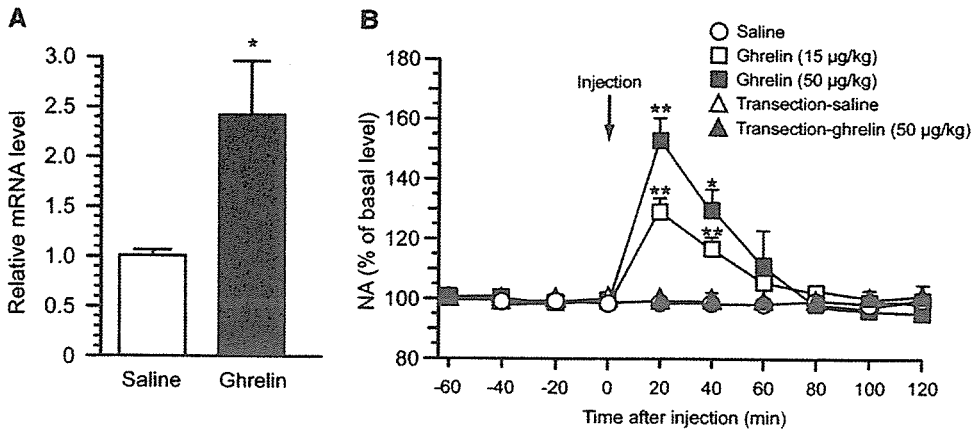

Figure 2. Ghrelin stimulates feeding via the NA system

A) DBH mRNA levels in rats receiving either ghrelin (15 μg/kg, i.v.) or saline. *$p < 0.03$ versus saline.

B) Effect of intravenous ghrelin on NA levels within the ARC in sham-treated and midbrain-transected rats. NA levels are represented as percentages of the mean concentration of NA in four consecutive dialysate samples taken before ghrelin injection. *$p < 0.01$, **$p < 0.0001$ versus sham saline.

Error bars represent the SEM.

neurons of the ARC at least partially via the vagal afferent pathway (Date et al., 2002). The possibility remains, however, that i.v. administered ghrelin may bind directly to receptors present on neurons in the ARC, as the ARC, situated at the base of the hypothalamus, is incompletely isolated from the general circulation by the blood-brain barrier (Banks and Kastin, 1985; Merchenthaler, 1991). The present study shows that ghrelin-induced feeding was abrogated in transected rats. This result indicates that neural pathways ascending from the NTS may play an important role in the transmission of ghrelin orexigenic signals to the hypothalamus. Conveyed to the NTS, these signals could be relayed to the hypothalamus through other transmitters produced by neurons located in the NTS.

NA system and peripheral ghrelin-induced feeding

Although afferent projections from the NTS to the hypothalamus are not exclusively noradrenergic, the noradrenergic pathway is the major constituent. We here showed that DBH mRNA levels increased significantly in the NTS after ghrelin (15 μg/kg) administration (Figure 2A). Considering that the NTS is the termination area of the vagal afferent fibers that receive vicerosensory information from the gastrointestinal tract, it seems reasonable to expect that peripheral ghrelin induces Fos expression in the NTS. We were not, however, able to detect any increase in the number of Fos-expressing neurons in the NTS (Date et al., 2005). This finding is consistent with previous data from other groups (Wang et al., 2002; Rüter et al., 2003). These results may depend on the fact that peripherally administered ghrelin decreases the firing rate of gastric vagal afferent fibers by binding to its receptor present in the vagal afferent terminals (Asakawa et al., 2001; Date et al., 2002). Thus, inhibitory signals caused by peripherally administered ghrelin may affect DBH expression in the NTS.

Peripherally administered ghrelin and synthetic GHSs primarily activate neurons located in the ARC (Hewson and Dickson, 2000). Most peripheral ghrelin-induced Fos-positive neurons in the ARC express NPY (Wang et al., 2002; Date et al., 2002). NPY and agouti-related protein (AgRP), which are colocalized in neurons of the ARC, have been implicated in the stimulation of feeding behavior. Pharmacological examinations indicated that centrally administered NPY Y-1 receptor antagonists block the orexigenic effect of ghrelin injected peripherally (Asakawa et al., 2001). Furthermore, Chen et al. demonstrated that peripherally administered ghrelin does not induce food intake in *NPY*$^{-/-}$, *AgRP*$^{-/-}$ double-knockout mice (Chen et al., 2004). These findings suggest that the ARC plays a crucial role in regulating peripheral ghrelin signals. In order to examine whether peripherally administered ghrelin affects the release of NA in the ARC, which is not only a noradrenergic terminal area but also a target site of peripheral ghrelin signals, we monitored overflow NA within or near the ARC using a microdialysis system. Overflow NA is thought to include both newly released NA and NA that was not subject to reuptake. Examination of overflow NA within or near the ARC after intravenous administration of 15 and 30 μg/kg ghrelin to sham-treated rats ($n = 7$ per group) revealed significantly increased NA concentrations within and near the ARC, reaching 129.7 ± 4.7% and 152.8 ± 7.5% of the control levels, respectively (Figure 2B). Ghrelin administration, however, did not induce NA release in transected rats. Hindbrain noradrenergic neurons innervating the hypothalamus are implicated in mediation of the feeding response to glucose deprivation (Ritter et al., 2001), suggesting that the NA system in the brain contributes significantly to feeding regulation and/or energy homeostasis. The present study demonstrates that ghrelin, an orexigenic signal produced in the periphery, increases DBH mRNA levels in the NTS and increases NA levels within the ARC. These results suggest that noradrenergic inputs, projecting from the hindbrain to the ARC, are critical for the feeding behavior induced by peripheral ghrelin. This study, however, has yet to elucidate whether peripheral ghrelin signals transmitted via the vagal afferent pathway affect the NA system in the ARC or whether ghrelin bound to the receptor present in the area postrema or NTS stimulates it. To clarify this issue, further examinations to evaluate NA overflow in the ARC of vagotomized animals are needed.

CCK, an anorectic peptide produced by the gastrointestinal tract, increases the firing rate of the vagal afferent fibers, and thereby transmits satiety information to the NTS. Recently, Sutton et al. showed that the CCK-induced reduction in feeding is modulated by a melanocortinergic pathway through extracellular signal-regulated kinase signaling in the NTS (Sutton

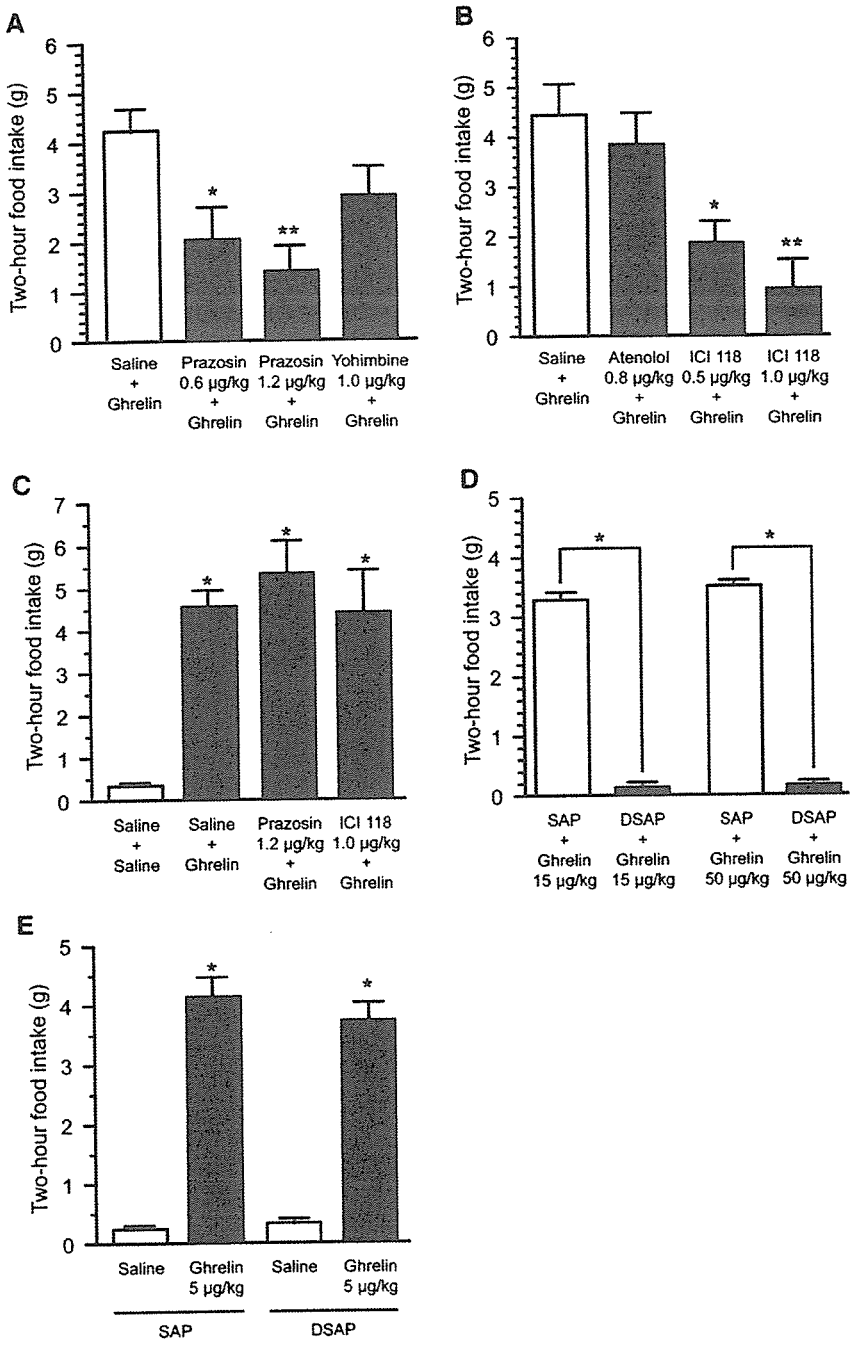

Figure 3. The effects of either pretreatment with adrenoceptor antagonists or disruption of DBH-containing neurons on ghrelin-induced feeding

A) Effect of i.c.v.-administered α_1 or α_2 antagonists on feeding induced by ghrelin (15 µg/kg). $^*p < 0.05$, $^{**}p < 0.005$ versus rats given saline plus ghrelin.

B) Effect of i.c.v.-administered β_1 or β_2 antagonists on feeding induced by ghrelin (15 µg/kg). $^*p < 0.005$, $^{**}p < 0.001$ versus rats given saline plus ghrelin.

C) Food intake of rats treated with an α_1 or a β_2 antagonist after a single intracerebroventricular administration of ghrelin (5 µg/kg). $^*p < 0.0005$ versus saline.

D) Effect of DSAP treatment on ghrelin-induced feeding. $^*p < 0.0001$.

E) Food intake of DSAP-treated rats after a single intracerebroventricular administration of ghrelin (5 µg/kg). $^*p < 0.0001$.

Error bars represent the SEM.

et al., 2005). There is also a report that fourth ventricular administration of the MC4-melanocortin receptor antagonist SHU9119 completely blocked the peripherally administered CCK-induced decrease in feeding (Fan et al., 2004). These findings indicated that the NTS is crucial for the integration of peripheral ascending signals with descending signals from the hypothalamus that relate to feeding. The precise molecular mechanisms that underlie the effect of peripheral ghrelin signals on NTS function remain to be elucidated. To fully understand the noradrenergic pathway from the NTS to the hypothalamus, further investigations into the identities of the intracellular signaling systems in the NTS that are mobilized by peripheral ghrelin, and the signals from the forebrain that modulate peripheral ghrelin signaling in the NTS are required.

NA can utilize at least four distinct receptor subtypes: α_1, α_2, β_1, and β_2 (O'Dowd et al., 1989). We examined which of these receptors was involved in ghrelin-induced feeding by treatment with an antagonist for each adrenoceptor. Ghrelin-induced feeding was attenuated in rats pretreated with either the specific α_1 antagonist prazosin or the specific β_2 antagonist ICI 118, but not the α_2 antagonist yohimbine or the β_1 antagonist atenolol (Figures 3A and 3B) (n = 7 per group). After injection of these adrenergic antagonists intracerebroventricularly (i.c.v.), rats were observed for behavioral signs of nausea (elongation of the body, gaping, raising the tail, and lowering the belly to the floor), ataxia, sedation, and anxiety (locomotion within the cage and avoidance of the front of the cage). The rats did not exhibit any of these signs during the testing period. We also tested

the orexigenic effect of centrally administered ghrelin in rats treated with prazosin or ICI 118, as these antagonists may nonspecifically suppress feeding in response to ghrelin. Centrally administered ghrelin increased feeding similarly in the prazosin- and ICI 118-treated groups and the control group (Figure 3C). This result suggests that although NA antagonists specifically suppressed feeding induced by peripherally administered ghrelin, centrally administered ghrelin induces feeding by a mechanism that is independent of the noradrenergic system. Considering that NA excites approximately 50% of the neurons in the ARC, probably due to a direct postsynaptic response through α_1- or β-adrenoceptors (Kang et al., 2000), peripherally administered ghrelin may activate NPY/AgRP neurons in the ARC through the NA system. A recent study also suggested the possibility that the GABAergic system is involved in ghrelin-induced feeding. Cowley et al. showed that ghrelin induced depolarization of ARC NPY neurons and hyperpolarization of ARC pro-opiomelanocortin (POMC) neurons using hypothalamic slices (Cowley et al., 2003). Given that NPY/AgRP neurons expressing are GABAergic, central ghrelin may induce the release of GABA from NPY axonal terminals and thereby modulate the activity of postsynaptic POMC neurons.

NA exerts a variety of responses that depend on the type of neurons and the expression of different adrenoceptor subtypes (Nicoll et al., 1990). Infusion of exogenous NA can cause either increases or decreases in food intake (references in Wellman, 2000), which may depend on the site of application or changes in the numbers of adrenoceptors according to the circadian cycle. For example, NA injection into the hypothalamic paraventricular nucleus (PVN) increases feeding through PVN α_2-adrenoceptors, whereas it decreases feeding through PVN α_1-adrennoceptors (Goldman et al., 1985; Wellman et al., 1993). The circadian pattern in the number of α_2-adrenoceptors within the PVN exhibits a sharp increase in α_2-adrenoceptors at the onset of the dark phase, a time when feeding is greatly enhanced. Taken together, it may be difficult to determine whether microinjection of an NA agonist or antagonist into the hypothalamic nuclei results in a physiologically significant effect. Therefore, in the present study, we focused on the role of endogenous NA induced by peripherally administered ghrelin in the control of food intake. We demonstrated that α_1- and β_2-receptor antagonists attenuated feeding induced by ghrelin. This result indicates that α_1- and/or β_2-adrenoceptors in the ARC play an important role in peripheral ghrelin-induced feeding.

To eliminate NA innervation of the ARC, we used DSAP, a monoclonal antibody specific for DBH, the enzyme that converts dopamine into NA, conjugated to saporin (SAP) (Fraley and Ritter, 2003). DSAP, an immunotoxin that allows an antibody against the NA synthetic enzyme DBH to selectively deliver the saporin toxin, can successfully destroy hindbrain neurons that contain DBH (Rinaman, 2003). Bilateral DSAP injections into the ARC induced an approximately 70% reduction in DBH-positive neurons in the NTS in comparison to the number of DBH neurons present in rats treated with an SAP control solution (data not shown). DSAP injections also completely disrupted peripherally administered ghrelin-induced feeding (Figure 3D) (n = 7 per group). We also tested the orexigenic effect of centrally administered ghrelin in the DSAP-treated rats. Centrally administered ghrelin increased feeding similarly in the DSAP-treated group and the control group (Figure 3E) (n = 7 per group). This finding suggests that the noradrenergic system in the ARC is not involved in centrally administered ghrelin-induced feeding.

There are several catecholaminergic neuronal cell groups in the hindbrain. DBH-positive neurons projecting to the hypothalamus are found within the A2 cell group located in the caudal medial and commissural NTS and the A1/C1 cell group located in the ventrolateral medulla (VML). Most NA neurons within the A2 group directly project to the hypothalamus, central nucleus of the amygdala, and bed nucleus of the stria terminalis, whereas the A2 NA neurons also project to these forebrain areas in part via the A1/C1 group. As viscerosensory signals from the gastrointestinal tract are carried to the caudal medial and commissural NTS via the vagal afferent pathway, NA neurons in A2 may be an integral component of the brainstem circuits that mediate ghrelin-induced feeding. Given the projection from the A2 group to the A1/C1 group, these integrative circuits would include a role for NA neurons in the VML. Our findings suggest that NA neurons in the hindbrain are necessary to convey ghrelin-related orexigenic signals to the hypothalamus.

Innervation of NPY neurons by DBH-containing fibers

To examine the effect of peripheral ghrelin signals ascending from the NTS on neurons in the ARC, we investigated DBH innervation and ghrelin-induced Fos expression using unilateral midbrain-transected rats as described previously (Ericsson et al., 1994; Sawchenko, 1988). We compared DBH innervation and Fos expression in the ARC ipsilateral and contralateral to the lesion. Midbrain transections significantly decreased the DBH-imunoreactive innervation ipsilateral to the lesion (Figures 4A and 4B). This finding is consistent with the fact that the ascending catecholamine input to the hypothalamus is largely unilateral. In lesioned rats, peripherally administered ghrelin resulted in a significant increase in Fos expression in the ARC that was contralateral to the lesion (ipsilateral side, 24.3 ± 1.8 neurons; contralateral side, 50.6 ± 1.9 neurons; $p < 0.001$) (Figures 4C and 4D). When saline was injected i.v. to lesioned rats, Fos expression did not differ significantly on the two sides of the brain (ipsilateral side, 11.6 ± 1.3 neurons; contralateral side, 11.9 ± 1.0 neurons; $p > 0.1$) (data not shown). These results suggest that the midbrain transections that were effective in reducing DBH-positive innervation blocked the response of neurons in the ARC to peripherally administered ghrelin.

Electron microscope immunohistochemistry demonstrated that NPY-immunoreactive perikaryon and dendritic process often received synapses from DBH-containing axon terminals (Figures 4E–4G). Approximately 40%–50% of hypothalamic NPY neuron innervation arises from catecholaminergic neurons in the hindbrain (Everitt and Hokfelt, 1989). NPY, a potent orexigenic peptide, is thought to be the final mediator of ghrelin feeding signals. To examine the anatomical linkage of NPY neurons, which are activated by ghrelin, with DBH-immunoreactive fibers, we performed immunohistochemistry. Intravenous ghrelin injection significantly increased Fos expression in 53% of the NPY neurons in the ARC (Figure 4H), in accordance with previous studies (Date et al., 2002). Triple labeling immunofluorescence demonstrated that 54% of these NPY neurons in the ARC induced to express Fos by ghrelin treatment were innervated by DBH-immunoreactive fibers (Figure 4I). These results suggest that ghrelin signals activate NPY neurons via the noradrenergic pathway ascending from the NTS to the ARC, resulting in increased feeding.

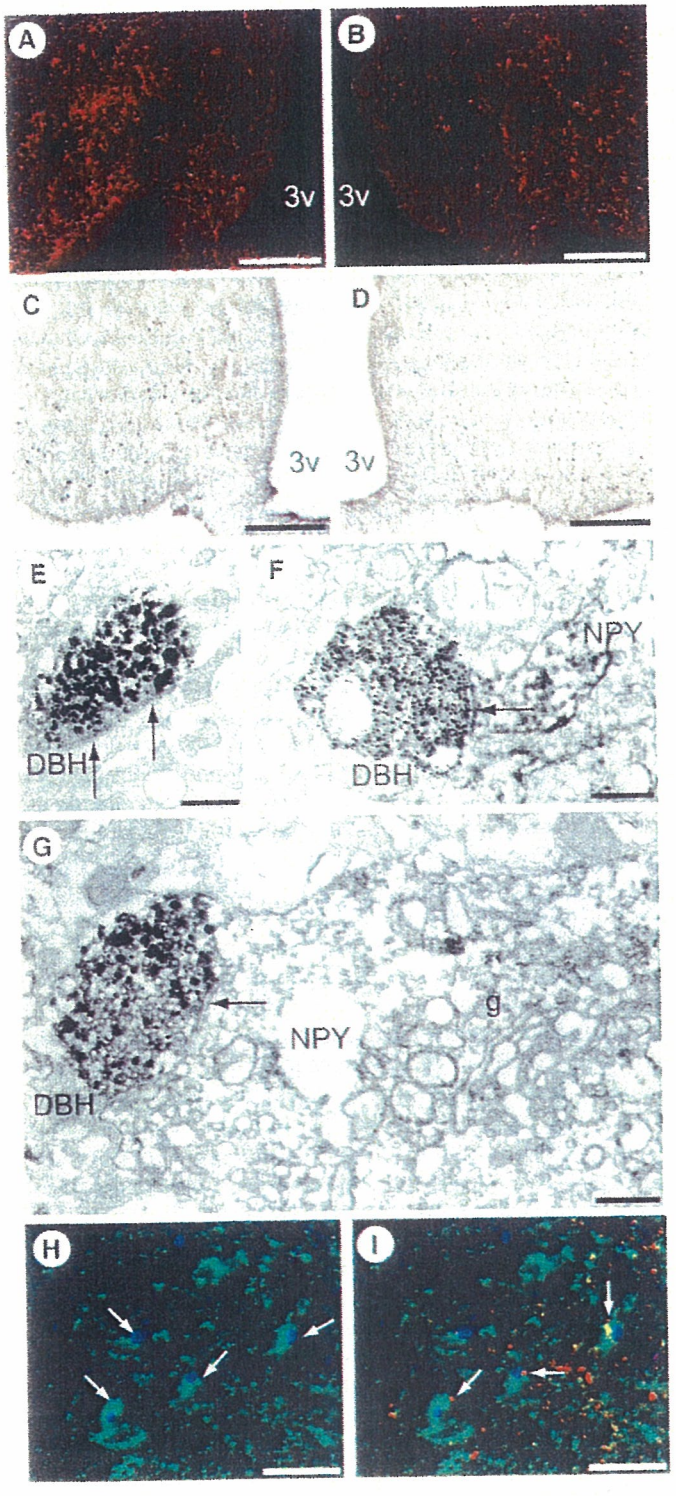

Figure 4. The effect of unilateral midbrain transections on ghrelin-induced Fos expression and activation of NPY neurons by ghrelin via the catecholaminergic pathways

A) DBH-immunoreactive fibers project to the ARC contralateral to the lesion.

B) DBH-immunoreactive innervation ipsilateral to the lesion decreases as compared to that on the contralateral side.

C) Peripherally administered ghrelin (15 μg/kg) induces Fos protein expression contralateral to the lesion.

D) Ghrelin-induced Fos expression ipsilateral to the lesion decreases as compared to that on the contralateral side.

E) DBH-immunoreactive axon terminal making synapses with immunonegative dendritic process (arrow, synapse).

F) DBH-immunoreactive axon terminal making synapses with NPY-immunoreactive dendritic process (arrow, synapse).

G) DBH-immunoreactive axon terminal making synapses with NPY-immunoreactive perikaryon (arrow, synapse).

H) Intravenous administration of ghrelin (15 μg/kg) upregulates Fos expression in NPY neurons of the ARC (arrows) (blue, Fos; green, NPY).

I) Fifty-four percent of ghrelin-activated NPY neurons receive projections from DBH-immunoreactive fibers (arrows) (blue, Fos; green, NPY; red, DBH). g; Golgi apparatus; 3v, third ventricle. The scale bar represents, respectively, 100 μm (**A and B**), 200 μm (**C and D**), 400 nm (**E–G**), and 50 μm (**H and I**).

The present study focused on the hypothesis that the neural pathway from the brainstem to the ARC plays a crucial role in transmitting peripheral ghrelin signals and peripheral ghrelin regulates feeding at least partially via NA-mediated neuronal transmission. Although the central circuits for feeding may have been altered in response to bilateral midbrain transections or DSAP treatment, the results shown here are consistent with the hypothesis. The hypothesis, if correct, is a counterpoint to the most widely accepted model for neuroendocrine energy balance regulation. We have shown previously that peripheral ghrelin-induced feeding is absent in either vagotomized or capsaicin-treated rats. We showed here that ghrelin-induced feeding is also canceled in midbrain transected rats. Thus, it may seem that peripheral ghrelin signals for starvation are transmitted to the hypothalamus only via the vagal afferent pathway and neural pathways from the NTS. However, we have to consider the possibility that vagotomy and/or midbrain transections affect several peripheral substances as well as central circuits relative to feeding. In addition, the present study has yet to address the direct relationship between peripheral ghrelin signals via the vagal afferent pathway and the NA system in the ARC. Taken together, it may be difficult to assert that peripheral ghrelin signals are transmitted only via the neural pathways. We, therefore, think that the humoral pathway and the neural pathway are important routes to convey peripheral energy balance information to the brain. Very recently, we found that peripherally administered leptin decreased 2 hr and 4 hr food intake in vagotomized, midbrain transected, and sham-operated rats, and the leptin-induced reduction in feeding was less pronounced in vagotomized and transected rats than in the sham-operated rats (unpublished data). These findings suggest that the vagal afferent pathway and/or the ascending efferent pathway from the brainstem to the hypothalamus are necessary elements for the effectual action of leptin on feeding and energy homeostasis. Feeding is regulated by a complicated interaction of many orexigenic and anorectic signals; sophisticated interactions between humoral pathways and neural pathways may be necessary to maintain energy homeostasis. We have shown that the central noradrenergic system is a candidate to mediate peripheral ghrelin signals. Although the pathways linking peripheral ghrelin to NA transmission are likely to be more complicated given the remarkable number of signals that provide input to the NTS and ARC, we believe that this study provides an important clue to understanding the feedback loops linking the brain and peripheral tissues in the control of feeding and energy homeostasis.

Experimental procedures

Experimental animals

We maintained male Wistar rats (Charles River Japan, Inc.), weighing 255.9 ± 2.0 g, under controlled temperature and light conditions (0800–2000 hr light).

For feeding and microdialysis experiments, an intravenous cannula was implanted into the right jugular vein of each rat under anesthesia. We performed unilateral or bilateral midbrain transections 5 days after implantation, as described details in the Supplemental Experimental Procedures. To confirm that the transection surgeries were successful, the brains were immunostained using an anti-DBH antiserum diluted 1:1000 (Chemicon International, Inc.) by the avidin-biotin complex method (Date et al., 1999) after the feeding tests were completed (Figure S3A). To facilitate the penetration of a microdialysis probe, a guide cannula (500 μm outside diameter; AG-12, Eicom) was stereotaxically implanted 1.0 mm above the ARC (0.2 mm lateral to the midline, 2.4 mm caudal to the bregma, and 9.0 mm ventral to the dura), fixed to the skull with acrylic dental cement, and sealed with a dummy cannula (350 μm external diameter; AD-12, Eicom). To inject adrenergic receptor antagonists into the rats, we implanted intracerebroventricular cannulae into the lateral cerebral ventricle. To block noradrenergic innervation of the ARC, we microinjected either a SAP-conjugated DBH-specific mouse monoclonal antibodies (DSAP; Advanced Targeting Systems; 42 ng/0.2 μl in phosphate buffer [pH 7.4], n = 6) or SAP-conjugated normal mouse IgG (SAP control solution) (Advanced Targeting Systems; 8.82 ng/0.2 μl, n = 6) bilaterally into the ARC (Ritter et al., 2001). Only animals exhibiting progressive weight gain after these surgeries were used in subsequent experiments. All procedures were performed in accordance with the Japanese Physiological Society's guidelines for animal care.

Food intake

First, rat ghrelin (Peptide Institute, Inc.) at 0.1–100 μg/kg (100 μl), or saline alone (100 μl) was administered i.v. at 1000 hr to ad libitum-fed rats that had undergone a sham operation (n = 7 per group). Second, rat ghrelin (15 or 50 μg/kg [100 μl]) was administered i.v. to rats that had undergone bilateral midbrain transection. Third, rat ghrelin (15 or 50 μg/kg [100 μl]) was administered i.v. to rats that had been treated with either DSAP or SAP control solution. Fourth, ghrelin (5 μg/kg [10 μl]) was injected i.c.v. at 1000 hr into rats that had undergone bilateral midbrain transections or sham operations, or into rats that had been treated with either DSAP or SAP control solution. The dose of centrally administered ghrelin (5 μg/kg) is often used as a standard while investigating the effect of i.c.v.-administered ghrelin on food intake under various conditions (Nakazato et al., 2001; Kamegai et al., 2000; Toshinai et al., 2003). Thus, this dosage is recognized as the most appropriate in constantly inducing food intake when administered i.c.v. Therefore, this dosage was also selected as a standard to evaluate i.c.v. administered ghrelin induced feeding. After ghrelin injection, rats were immediately returned to their cages. Two hour food intake was then measured.

Quantitative RT-PCR

Two hours after intravenous administration of ghrelin (15 μg/kg) or saline to rats, total RNA was extracted from the NTS using TRIZOL Reagent (Invitrogen Corp.). Quantitative RT-PCR for DBH was conducted with a LightCycler system (Roche Diagnostics) using a LightCycler-Fast Start DNA Master SYBR Green I kit (Roche) and the following primer set for rat DBH: 5′-CTAGGGCCCTGGGCGCCAAGGCATT-3′ and 5′-GCCAGAGGAGTCGCG CCGGCCTT-3′. Known amounts of DBH cDNA were used to obtain a standard curve. Rat rRNA levels were also measured as an internal control.

Microdialysis

One week after midbrain transection, the rats were lightly anesthetized with isoflurane, and the dummy cannula was replaced with a microdialysis probe. The tip of the microdialysis probe, covered with hollow fibers (1.0 mm in length, 220 μm external diameter, regenerated cellulose membrane with a molecular weight cutoff of 48 kDa; Eicom), was set to extend 1 mm beyond the guide cannula to reach the ARC. Microdialysis was performed under free-moving conditions. A microinfusion pump was used to continually perfuse the probe with modified physiological Ringer's solution (147 mM NaCl, 4 mM KCl, and 2.3 mM $CaCl_2$ [pH 6.5]) at a constant flow rate of 1 μl/min. To measure NA, chromatographic analysis of dialysates was carried out by HPLC with electrochemical detection as described previously (Ishizuka et al., 2000). The perfusate from the ARC was automatically injected into the HPLC every 20 min. After a 3 hr stabilization period, baseline NA levels were assessed in four consecutive dialysate samples. At the end of each experiment, rats were sacrificed with an overdose of pentobarbital sodium; the brains were then fixed in 10% neutral buffered formalin. Placement of the microdialysis probe was verified histologically in 40-μm cresyl violet-stained coronal sections (Figure S3B).

Effect of adrenoceptor blockers on ghrelin-induced feeding

At 0930 hr, rats were i.c.v. administered either vehicle alone (saline, n = 6) or one of the specified adrenergic receptor antagonists: prazosin (selective α_1 antagonist: 0.6 or 1.2 μg/kg, n = 6 each) (Sigma Chemical Co.), yohimbine (selective α_2 antagonist: 1.0 μg/kg, n = 6) (Sigma), atenolol (selective β_1 antagonist: 0.8 μg/kg, n = 10) (Sigma), or ICI 118 (selective β_2 antagonist: 0.5 or 1.0 μg/kg, n = 6 each) (Sigma). Thirty minutes after adrenergic receptor antagonist injection, ghrelin (50 μg/kg) was administered intraperitoneally to rats; 2 hr food intake was measured. We also tested the orexigenic effect of centrally administered ghrelin in rats that had been injected with prazosin or ICI 118. Thirty minutes after prazosin (1.2 μg/kg, n = 6) or ICI 118 (1.0 μg/kg, n = 6) injection, ghrelin (5 μg/kg) was administered i.c.v. to rats; 2 hr food intake was measured. The rats fasted between the two injections.

Immunohistochemistry

Ghrelin (15 μg/kg) or saline was injected i.v. into rats 90 min before transcardial perfusion with fixative containing 4% paraformaldehyde (n = 5 per group). The brains of animals were then cut into 20-μm thick sections. The sections were first incubated with anti-c-Fos antiserum (1:500, Santa Cruz Biotechnology), and then with Alexa Flour 350-conjugated donkey anti-goat IgG (Molecular Probes, Inc.). Next, samples were incubated with anti-NPY antiserum (1:500, ImmunoStar, Inc.), then with Alexa Flour 488-conjugated chicken anti-rabbit IgG (Molecular Probes, Inc.). Finally, the samples were incubated with anti-DBH antiserum (1:1,000, Chemicon International, Inc.), then with Alexa Flour 568-conjugated goat anti-mouse IgG (Molecular Probes, Inc.). Samples were then observed under a BH2-RFC microscope (Olympus Corp.). We counted the number of Fos-immunoreactive cells in the bilateral ARCs (bregma: −2.30 to −3.30 from Paxinos and Watson's rat brain atlas). Sections from unilaterally transected rats were also incubated with anti-DBH antiserum, and then with Alexa Flour 568-conjugated goat anti-mouse IgG (Molecular Probes, Inc.). A significant (>60%) depletion of DBH-immunoreactive fibers was determined by semi-quantitative comparison of the strength of the DBH-positive innervation of the ARC ipsilateral and contralateral to the lesion by two independent observers (Sawchenko, 1988). Sections from unilaterally transected rats were incubated with anti-c-Fos antiserum (Santa Cruz Biotechnology), and then stained by the avidin-biotin complex method (Date et al., 1999). The number of Fos-immunoreactive cells was compared in the ARC ipsilateral and contralateral to the letion. Fos-expressing cells of the ARC in a 0.7-mm right triangle (0.245 mm^2) were counted in every fifth section (ten tissue sections per rat) using a cell-counting program written for NIH Image (v1.62; NIH).

Electron microscope immunohistochemistry

Three Wistar rats were perfused as described above. The brain was cut into 30–40 μm thick sections using an Oxford vibratome (Oxford Instruments). Electron microscope immunohistochemistry was performed using anti-NPY antiserum and anti-DBH antiserum as described previously (Toshinai et al., 2003).

Statistical analysis

We analyzed groups of data (means ± SEM) using analysis of variance (ANOVA) and post hoc Fisher tests. p values less than 0.05 were considered to be significant (two-tailed tests).

Supplemental data

Supplemental Data include Supplemental Results, Supplemental Experimental Procedures, Supplemental References, and three figures and can be found with this article online at http://www.cellmetabolism.org/cgi/content/full/4/4/323/DC1/.

Acknowledgments

We thank Rie Matsuura, Tomoko Tsuruta, and Yuko Nobe for their assistance. This study was supported in part by the 21st Century Center of Excellence Program (COE), the Program for Promotion of Fundamental Studies in Health Sciences of the National Institute of Biomedical Innovation (NIBIO),

and by grants-in-aid from the Ministry of Education, Culture, Sports, Science, and Technology of Japan and the Ministry of Health, Labor, and Welfare of Japan.

Received: October 15, 2005
Revised: July 19, 2006
Accepted: September 13, 2006
Published online: October 3, 2006

References

Abbott, C.R., Monteiro, M., Small, C.J., Sajedi, A., Smith, K.L., Parkinson, J.R., Ghatei, M.A., and Bloom, S.R. (2005). The inhibitory effects of peripheral administration of peptide YY(3-36) and glucagon-like peptide-1 on food intake are attenuated by ablation of the vagal-brainstem-hypothalamic pathway. Brain Res. *1044*, 127–131.

Asakawa, A., Inui, A., Kaga, T., Yuzuriha, H., Nagata, T., Ueno, N., Makino, S., Fujimiya, M., Niijima, A., Fujino, M.A., et al. (2001). Ghrelin is an appetite-stimulatory signal from stomach with structural resemblance to motilin. Gastroenterology *120*, 337–345.

Banks, W.A., and Kastin, A.J. (1985). Permeability of the blood-brain barrier to neuropeptides: the case for penetration. Psychoneuroendocrinology *10*, 385–399.

Chen, H.Y., Trumbauer, M.E., Chen, A.S., Weingarth, D.T., Adams, J.R., Frazier, E.G., Shen, Z., Marsh, D.J., Feighner, S.D., Guan, X.M., et al. (2004). Orexigenic action of peripheral ghrelin is mediated by neuropeptide Y and agouti-related protein. Endocrinology *145*, 2607–2612.

Cowley, M.A., Smith, R.G., Diano, S., Tschöp, M., Pronchuk, N., Grove, K.L., Strasburger, C.J., Bidlingmaier, M., Esterman, M., Heiman, M.L., et al. (2003). The distribution and mechanism of action of ghrelin in the CNS demonstrates a novel hypothalamic circuit regulating energy homeostasis. Neuron *37*, 649–661.

Crawley, J.N., Kiss, J.Z., and Mezey, E. (1984). Bilateral midbrain transections block the behavioral effects of cholecystokinin on feeding and exploration in rats. Brain Res. *322*, 316–321.

Date, Y., Ueta, Y., Yamashita, H., Yamaguchi, H., Matsukura, S., Kangawa, K., Sakurai, T., Yanagisawa, M., and Nakazato, M. (1999). Orexins, orexigenic hypothalamic peptides, interact with autonomic, neuroendocrine and neuroregulatory systems. Proc. Natl. Acad. Sci. USA *96*, 748–753.

Date, Y., Kojima, M., Hosoda, H., Sawaguchi, A., Mondal, M.S., Suganuma, T., Matsukura, S., Kangawa, K., and Nakazato, M. (2000). Ghrelin, a novel growth hormone-releasing acylated peptide, is synthesized in a distinct endocrine cell type in the gastrointestinal tracts of rats and humans. Endocrinology *141*, 4255–4261.

Date, Y., Murakami, N., Toshinai, K., Matsukura, S., Niijima, A., Matsuo, H., Kangawa, K., and Nakazato, M. (2002). The role of the gastric afferent vagal nerve in ghrelin-induced feeding and growth hormone secretion in rats. Gastroenterology *123*, 1120–1128.

Date, Y., Toshinai, K., Koda, S., Miyazato, M., Shimbara, T., Tsuruta, T., Niijima, A., Kangawa, K., and Nakazato, M. (2005). Peripheral interaction of ghrelin with cholecystokinin on feeding regulation. Endocrinology *146*, 3518–3525.

Dornonville de la Cour, C., Björkqvist, M., Sandvik, A.K., Bakke, I., Zhao, C.-M., Chen, D., and Håkanson, R. (2001). A-like cells in the rat stomach contain ghrelin and do not operate under gastrin control. Regul. Pept. *99*, 141–150.

Ericsson, A., Kovacs, K.J., and Sawchenko, P.E. (1994). A functional anatomical analysis of central pathways subserving the effects of interleukin-1 on stress-related neuroendocrine. J. Neurosci. *14*, 897–913.

Everitt, B.J., and Hokfelt, T. (1989). The coexistence of neuropeptide Y with other peptides and amines in the central nervous system. In Neuropeptide Y., V. Mutt, K. Fuxe, T. Hokfelt, and J. Lundberg, eds. (New York: Raven Press), pp. 61–72.

Fan, W., Ellacott, K.L., Halatchev, I.G., Takahashi, K., Yu, P., and Cone, R.D. (2004). Cholecystokinin-mediated suppression of feeding involves the brainstem melanocortin system. Nat. Neurosci. *7*, 335–336.

Fraley, G.S., and Ritter, S. (2003). Immunolesion of norepinephrine and epinephrine afferents to medial hypothalamus alters basal and 2-deoxy-D-glucose-induced neuropeptide Y and agouti gene-related protein messenger ribonucleic acid expression in the arcuate nucleus. Endocrinology *144*, 75–83.

Goldman, C.K., Marino, L., and Leibowitz, S.F. (1985). Postsynaptic alpha 2-noradrenergic receptors mediate feeding induced by paraventricular nucleus injection of norepinephrine and clonidine. Eur. J. Pharmacol. *115*, 11–19.

Grill, H.J., and Smith, G.P. (1988). Cholecystokinin decreases sucrose intake in chronic decerebrate rats. Am. J. Physiol. *254*, R853–R856.

Grill, H.J., and Norgren, R. (1978). The taste reactivity test. II. Mimetic responses to gustatory stimuli in chronic thalamic and chronic decerebrate rats. Brain Res. *143*, 281–297.

Hewson, A.K., and Dickson, S.L. (2000). Systemic administration of ghrelin induces Fos and Egr-1 proteins in the hypothalamic arcuate nucleus of fasted and fed rats. J. Neuroendocrinol. *12*, 1047–1049.

Ishizuka, Y., Ishida, Y., Jin, Q., Kato, K., Kunitake, T., Mitsuyama, Y., and Kannan, H. (2000). Differential profiles of nitric oxide and norepinephrine releases in the paraventricular nucleus region in response to mild footshock in rats. Brain Res. *862*, 17–25.

Kamegai, J., Tamura, H., Shimizu, T., Ishii, S., Sugihara, H., and Wakabayashi, I. (2000). Central effect of ghrelin, an endogenous growth hormone secretagogue, on hypothalamic peptide gene expression. Endocrinology *141*, 4797–4800.

Kang, Y.M., Ouyang, W., Chen, J.Y., Qiao, J.T., and Dafny, N. (2000). Norepinephrine modulates single hypothalamic arcuate neurons via α_1 and β adrenergic receptors. Brain Res. *869*, 146–157.

Koda, S., Date, Y., Murakami, N., Shimbara, T., Hanada, T., Toshinai, K., Niijima, A., Furuya, M., Inomata, N., Osuye, K., et al. (2005). The role of the vagal nerve in peripheral PYY_{3-36}-induced feeding reduction in rats. Endocrinology *146*, 2369–2375.

Kojima, M., Hosoda, H., Date, Y., Nakazato, M., Matsuo, H., and Kangawa, K. (1999). Ghrelin is a novel growth hormone releasing acylated peptide from stomach. Nature *402*, 656–660.

Merchenthaler, I. (1991). Neurons with access to the general circulation in the central nervous system of the rat: a retrograde tracing study with fluoro-gold. Neuroscience *44*, 655–662.

Nakazato, M., Murakami, N., Date, Y., Kojima, M., Matsuo, H., Kangawa, K., and Matsukura, S. (2001). A role for ghrelin in the central regulation of feeding. Nature *409*, 194–198.

Nicoll, R.A., Malenka, R.C., and Kauer, J.A. (1990). Functional comparison of neurotransmitter receptor subtypes in mammalian central nervous system. Physiol. Rev. *70*, 513–565.

O'Dowd, B.F., Lefkowitz, R.J., and Caron, M.G. (1989). Structure of the adrenergic and related receptors. Annu. Rev. Neurosci. *12*, 67–83.

Rinaman, L. (2003). Hindbrain noradrenergic lesions attenuate anorexia and alter central cFos expression in rats after gastric viscerosensory stimulation. J. Neurosci. *23*, 10084–10092.

Ritter, S., Bugarith, K., and Dinh, T.T. (2001). Immunotoxic destruction of distinct catecholamine subgroups produces selective impairment of glucoregulatory responses and neuronal activation. J. Comp. Neurol. *432*, 197–216.

Rüter, J., Kobelt, P., Tebbe, J.J., Avsar, Y., Veh, R., Wang, L., Klapp, B.F., Wiedenmann, B., Taché, Y., and Monnikes, H. (2003). Intraperitoneal injection of ghrelin induces Fos expression in the paraventricular nucleus of the hypothalamus in rats. Brain Res. *991*, 26–33.

Sawchenko, P.E., and Swanson, L.W. (1981). Central noradrenergic pathways for the integration of hypothalamic neuroendocrine and autonomic responses. Science *214*, 685–687.

Sawchenko, P.E. (1988). Effect of catecholamine-depleting medullary knife cuts on corticotropin-releasing factor and vasopressin immunoreactivity in the hypothalamus of normal and steroid-manipulated rats. Neuroendocrinology *48*, 459–470.

Smith, G.P., Jerome, C., Cushin, B.J., Eterno, R., and Simansky, K.J. (1981). Abdominal vagotomy blocks the satiety effect of cholecystokinin in the rat. Science *213*, 1036–1037.

Sutton, G.M., Duos, B., Patterson, L.M., and Berthoud, H.R. (2005). Melanocortinergic modulation of cholecystokinin-induced suppression of feeding through extracellular signal-regulated kinase signaling in rat solitary nucleus. Endocrinology *146*, 3739–3747.

Toshinai, K., Date, Y., Murakami, N., Shimada, M., Mondal, M.S., Shimbara, T., Guan, J.L., Wang, Q.P., Funahashi, H., Sakurai, T., et al. (2003). Ghrelin-induced food intake is mediated via the orexin pathway. Endocrinology *144*, 1506–1512.

Tschöp, M., Smiley, D.L., and Heiman, M. (2000). Ghrelin induces adiposity in rodents. Nature *407*, 908–913.

Wang, L., Saint-Pierre, D.H., and Taché, Y. (2002). Peripheral ghrelin selectively increases Fos expression in neuropeptide Y - synthesizing neurons in mouse hypothalamic arcuate nucleus. Neurosci. Lett. *325*, 47–51.

Wellman, P.J., Davies, B.T., Morien, A., and McMahon, L. (1993). Modulation of feeding by hypothalamic paraventricular nucleus α_1- and α_2-adrenergic receptors. Life Sci. *53*, 669–679.

Wellman, P.J. (2000). Norepinephrine and the control of food intake. Nutrition *16*, 837–842.

Wren, A.M., Small, C.J., Ward, H.L., Murphy, K.G., Dakin, C.L., Taheri, S., Kennedy, A.R., Roberts, G.H., Morgan, D.G.A., Ghatei, M.A., and Bloom, S.R. (2000). The novel hypothalamic peptide ghrelin stimulates food intake and growth hormone secretion. Endocrinology *141*, 4325–4328.

Available online at www.sciencedirect.com
SCIENCE DIRECT®
Biochemical and Biophysical Research Communications 345 (2006) 377–384
BBRC
www.elsevier.com/locate/ybbrc

Structural and functional analogs of the novel mammalian neuropeptide, neuromedin S (NmS), in the dermal venoms of Eurasian bombinid toads

Tianbao Chen [a], Mei Zhou [a], Brian Walker [a], Pat Harriot [b], Kenji Mori [c], Mikiya Miyazato [c], Kenji Kangawa [c], Chris Shaw [a,*]

[a] *Schools of Pharmacy, Queen's University, Belfast BT9 7BL, Northern Ireland, UK*
[b] *Biology and Biochemistry, Queen's University, Belfast BT9 7BL, Northern Ireland, UK*
[c] *Department of Biochemistry, National Cardiovascular Center Research Institute, 5-7-1 Fujishirodai, Suita, Osaka 565-8565, Japan*

Received 13 April 2006
Available online 2 May 2006

Abstract

We report the isolation and structural characterization of two neuromedin S (NmS) analogs, (NmS-17 and NmS-33), from the dermal venoms of Eurasian bombinid toads. NmS is a novel neuromedin U (NmU)-related peptide with potent anorexigenic and circadian rhythm-modulating properties recently discovered in mammals. Cloning of NmS precursor-encoding cDNAs from skin venom-derived libraries revealed the presence of a high degree of transcript splice variation comparable to that found previously for NmU in both amphibian skin and mammalian brain. Synthetic replicates of both amphibian NmS peptides evoked robust and dose-dependent transient increases in intracellular calcium ion concentrations in CHO cells that had been stably transfected with either FM-3/GPR66 or FM-4/TGR-1 human NmU receptors. The potency and efficacy of these amphibian skin peptides at such receptors were comparable to those observed with human NmS and rat NmS. These data show that NmS and NmU genes had already diverged at the level of the Amphibia and that differential splicing of their transcribed mRNAs has been highly conserved throughout tetrapod vertebrate evolution indicative of fundamental biological function. NmS is additionally a novel neuropeptide homolog that can be added to the biologically active peptide arsenal of amphibian venom/defensive skin secretions.

Keywords: Amphibian; Venom; Peptide; Neuromedin; Cloning

Neuromedin U (NmU) was isolated by one of the present co-authors (K.K.) in 1985 from an extract of hog spinal cord due to its hypertensive and uterine smooth muscle contracting properties [1]. Two molecular forms were isolated and were designated as NmU-25 and NmU-8, the latter representing the biologically active C-terminal core of the former. NmU was found to have a classical brain-gut distribution and to be of ubiquitous occurrence in a wide range of vertebrates including human, dog, rat, guinea pig, rabbit, chicken, and frog [2–9]. In a variety of bioassays, NmU was found to possess additional peripheral biological effects including modification of intestinal ion transport, adrenocortical function, and splanchnic blood flow [10–12]. However, intracerebroventricular administration of the peptide into rats induced a significant reduction in food intake (anorexigenic effect), augmentation of stress responses, and elevations in body temperature and heart rate [13–15].

Amphibian venoms/defensive skin secretions are rich sources of biologically active peptides many of which are structural and functional homologs of endogenous vertebrate neuropeptides leading several authors to speculate that every vertebrate neuropeptide may have a frog skin secretion equivalent [16,17]. In 2000, we reported the presence of an NmU homolog in the defensive skin secretion of the Australasian tree frog, *Litoria caerulea* [18]. This

* Corresponding author. Fax: +44 2890 247794.
E-mail address: chris.shaw@qub.ac.uk (C. Shaw).

0006-291X/$ - see front matter © 2006 Elsevier Inc. All rights reserved.
doi:10.1016/j.bbrc.2006.04.103

peptide, designated NmU-23, was found to exhibit full-NmU agonist activity in preparations of rat uterine and human urinary bladder smooth muscle and to be equipotent with NmU-25 in displacing this radiolabeled ligand in a rat uterine smooth muscle membrane radioreceptor assay. Subsequently, the cDNA encoding this peptide was cloned from a library manufactured from lyophilized skin secretion of this tree frog using a novel technique developed in our laboratory [19]. In addition to the full-length preproneuromedin U transcript, deemed to be such due to its alignment with the homologous human transcript cloned from a pituitary gland library, we identified a number of splice variants largely involving splicing events within short exons immediately upstream of the NmU encoding sequence. This prompted a study of frog, rat, and human brain in which the same splice variation was observed. Thus within the tetrapod vertebrates, the NmU gene appears to possess a multiplicity of short exons within the open-reading frame that undergoes a highly conserved and discrete differential regional splicing indicative of an as yet unidentified but presumably fundamental function.

Recently, a second NmU-related peptide, designated neuromedin S (NmS), has been identified in and isolated from rat, mouse, and human brain tissues [20]. This was achieved by reverse deorphanization of the NmU receptors, FM-3/GPR66, and FM-4/TGR-1, stably transfected into CHO cells, and interrogated with brain peptide extracts using a calcium mobilization assay. Using radioimmunoassay systems that employ phylogenetically conserved, site-specific antisera to neuropeptides, we have screened reverse phase HPLC-fractionated venoms/defensive skin secretions from some 140 different species of amphibians for at least 20 neuropeptides. In this screen, we confirmed the presence of NmU immunoreactivity in *L. caerulea* skin secretion [18], although this was somewhat heterogenous indicating the presence of molecular forms in addition to the major NmU-23. In addition, we detected NmU immunoreactivity in a closely related species, the white-lipped tree frog, *Litoria infrafrenata*. What was most surprising was the presence of NmU immunoreactivity in skin secretion fractions of the three species of bombinid toad subjected to analysis. All other species were consistently negative. Structural and bioinformatic analyses of the bombinid toad immunoreactive peptides indicated that they were in fact NmS homologs. Molecular cloning of these toad skin NmS cDNAs from venom-derived libraries revealed a spectrum of splice variants that reflected our previous findings for NmU transcripts in *L. caerulea* skin secretion [19]. Synthetic replicates of frog NmS-17 and frog NmS-33 interacted with stably transfected GPR66 and TGR-1 NmU receptors in a manner similar to endogenous human and rat NmS homologs. These data demonstrate, for the first time, that NmU and NmS genes had already diverged within the amphibians and that the systematic study of amphibian defensive skin secretions can provide many valuable insights into the molecular evolution of vertebrate regulatory peptides.

Materials and methods

Acquisition of skin secretions. Young adult specimens of the Oriental fire-bellied toad (*Bombina orientalis*, $n = 5$), the Chinese giant fire-bellied toad (*Bombina maxima*, $n = 3$), and the European yellow-bellied toad (*Bombina variegata*, $n = 10$) were captive-bred and were maintained in separate species terraria at a temperature of 22 °C under a 12 h/12 h light/dark cycle with three feeds of multi-vitamin loaded crickets per week. Following a 12-week period of acclimatization, venom was obtained by gentle transdermal electrical stimulation (4-ms pulse width, 50 Hz, 5–7 V) of deionized water-moistened skin for three periods of 15 s duration [21]. The viscous white granular gland secretions were washed from the skins of the toads using a stream of deionized water into pre-chilled (2 °C) glass beakers, snap-frozen in liquid nitrogen, and lyophilized. The secretions from each of the three species of toads were separately pooled. Approximately 10–15 mg dried weight of skin secretion could be obtained from each specimen on a monthly basis.

Reverse phase HPLC/MS. Ten milligrams of lyophilized venom from each species of toad were separately subjected to reverse phase HPLC/MS analysis using a gradient formed from 0.05/99.95 (v/v) trifluoroacetic acid (TFA)/water to 0.05/39.95/60.0 (v/v/v) TFA/water/acetonitrile in 60 min at a flow rate of 1 ml/min. A Thermoquest gradient reversed phase HPLC system, fitted with an analytical column (Phenomenex, C-18, 25 × 0.45 cm), and interfaced with a Thermoquest LCQ™ Deca electrospray ion-trap mass spectrometer was employed. The effluent from the chromatographic column was flow-split with approximately 10% entering the mass spectrometer source and 90% directed towards a fraction collector. Dead volume between column and fraction collector was minimal (20 µl). The molecular masses of polypeptides in each chromatographic fraction were further analyzed using matrix-assisted laser desorption/ionization, time-of-flight mass spectrometry (MALDI-TOF MS) on a linear time-of-flight Voyager DE PRO mass spectrometer (Perseptive Biosystems, MA, USA) in positive detection mode using α-cyano-4-hydroxycinnamic acid as the matrix. Internal mass calibration of the instrument with known standards established the accuracy of mass determination as ±0.1%. The peptides possessing masses coincident with those of NmS analogs deduced from cloned cDNAs were each subjected to primary structural analyses by automated Edman degradation using an Applied Biosystems 491 Procise sequencer in pulsed-liquid mode or by MS/MS fragmentation sequencing using the LCQ™ Deca electrospray ion-trap instrument.

Analysis of reverse phase HPLC fractions by NmU/NmS radioimmunoassay. Fifty microliter samples from each chromatographic fraction were removed and lyophilized prior to radioimmunometric analysis using a system described in detail previously [18]. Briefly, antiserum GP 9320 was raised in a guinea pig immunized with a (Lys^0)-NmU-8/glutaraldehyde/ovalbumin conjugate. The assay buffer, in which all reactants were diluted, consisted of 0.04 M sodium phosphate, pH 7.2, containing 0.14 M sodium chloride and 2% (v/v) horse serum. The assay volume was 400 µl consisting of 100 µl of diluted NmU-8 antiserum (1:38,000), 100 µl of monoradioiodinated NmU-8 tracer (100 Bq; 2 fmol), and 100 µl of NmU-8 standard (0–250 fmol/ml) or unknown sample. Addition of tracer was delayed for 24 h and bound/free tracer was separated after a further 24 h by addition of 1 ml of 0.05% dextran-coated microfine charcoal and centrifugation at 1100*g* for 30 min. All procedures were carried out at 4 °C and under the conditions described, the sensitivity of the assay, defined as the least amount that could be detected above zero with 95% confidence, was 1.2 fmol NmU-8/assay tube. The antiserum cross-reacted fully on a molar basis with NmU-8, NmU-25, frog NmU-23, human NmS, and rat NmS but exhibited no cross-reactivity with a wide range of vertebrate neuropeptides.

Cloning of NmS precursor cDNAs from venom-derived libraries. Five milligrams of lyophilized venom from each species were dissolved separately in 1 ml of cell lysis/mRNA stabilization buffer (Dynal Biotec, UK). Polyadenylated mRNA was isolated from the stabilization buffer/skin secretion mixtures using magnetic oligo(dT) beads as described by the

manufacturer (Dynal Biotec, UK) and reverse-transcribed. The cDNA was subjected to 3′- and 5′-RACE procedures to obtain full-length prepro-NmS nucleic acid sequence data using a SMART-RACE kit (Clontech UK) essentially as described by the manufacturer. Briefly, the 3′-RACE reactions employed an NUP primer (supplied with the kit) and a degenerate sense primer (NmS-S1; 5′-GGIATHGTIGGIMGICCITT-3′) that was complementary to the internal amphibian NmS amino acid sequence, –GIVGRPF–. 3′-RACE products were gel-purified and cloned using a pGEM-T vector system (Promega Corporation) and sequenced using an ABI 3100 automated DNA sequencer. The sequence data obtained from these 3′-RACE products were used to design a gene-specific primer, (NmS-AS1: 5′-TGTGTCCATAAGATCAGGCAGAAT-3′) to a sequence within the 3′-non-translated region. 5′-RACE reactions were performed using this primer in conjunction with the NUP and the resultant products were gel-purified, cloned, and sequenced as described above. Following acquisition of these data, a second gene-specific sense primer (NmS-S2: 5′-CCTCTACCACTGCTGCTTGCGATC-3′) was designed to a site within the putative signal peptide domain and was employed in 3′-RACE reactions. Products were likewise gel-purified, cloned, and sequenced as described previously. All identified sequences and splice variants were represented at least ten times in the several hundred clones that were sequenced.

Chemical synthesis of toad NmS-17 and NmS-33. Subsequent to unequivocal primary structural characterization of the toad defensive secretion peptides NmS-17 and NmS-33, each was separately synthesized using solid-phase Fmoc chemistry and an Applied Biosystems 433 peptide synthesizer. Following cleavage from the resin and deprotection, each respective peptide was purified by reverse phase HPLC, a process that was monitored and quality-controlled by means of electrospray mass spectrometry using an LCQ DECA instrument (Thermo-Electron Corporation, San Jose, CA, USA).

Production of human NmU-receptor transfected cell lines. CHO cells were stably transfected with either human FM-3/GPR66 (GenBank Accession No. BC036543) or with FM-4/TGR-1 (AF242874) NmU/NmS receptors by cloning into pcDNA3.1 vectors. The cell lines (CHO/FM-3-14 and CHO/FM-4-16), that exhibited the greatest elevations in free cytosolic Ca^{2+} ion concentrations when challenged with human NmU, were used in this study. The intracellular calcium mobilization assay was performed using a FLIPR system (Molecular Devices) that has been described in detail previously [20]. All peptide solutions contained 1% (w/v) bovine serum albumin and each synthetic peptide was subjected to amino acid analysis prior to construction of solutions for dose–response studies.

Results

Identification and structural characterization of toad venom NmS peptides

NmS/NmU immunoreactive peptides were identified in reverse phase HPLC fractions of venom from each of the three species of bombinid toad investigated. The profile obtained with *B. orientalis* is shown in Fig. 1. Two immunoreactive peptides were resolved in fractions of *B. maxima* and *B. orientalis* venoms in contrast to the single peptide in *B. variegata* that was coincident in retention time with the more abundant and hydrophilic peptide resolved in the other congeneric species. This more hydrophilic peptide was found to be of identical molecular mass (1964 Da—non-protonated) in all three species. A combination of automated Edman degradation and MS/MS fragmentation sequencing established the primary structure as: DSSGIVGRPFFLFR PRNamide. The minor, and more hydrophobic peptides from *B. maxima* and *B. orientalis* were found to be of similar (3800 and 3818 Da—non-protonated, respectively) but not identical molecular masses. The primary structure of the *B. maxima* peptide was established by automated Edman degradation as: FLFQFSRAKDPSLKIGDSSGIVGRPF FLFRP(RNamide). The last C-terminal amino acid residues were not detectable in the final cycles of Edman degradation but their inclusion matched the previously observed molecular mass of this peptide. The *B. orientalis* peptide was also subjected to automated Edman degradation and the two C-terminal residues were likewise not detected. However, as in the first instance, their inclusion provided an exact match to observed molecular mass. The *B. orientalis* peptide differed in primary structure from the *B. maxima* homolog at two sites—a Thr for Ala substitution at position 8 and a Thr for Ile substitution at position 15. This finding explained the discrepancy in molecular mass observed between the two

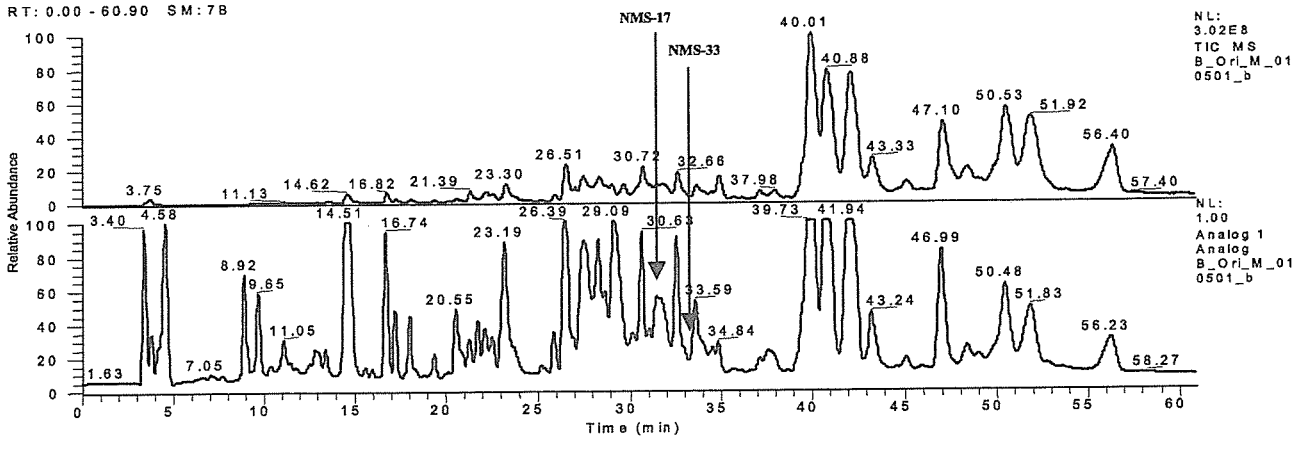

Fig. 1. A typical LC/MS spectrogram of skin venom from the Oriental fire-bellied toad, *B. orientalis*. The upper panel illustrates total ion count entering the mass spectrometer and the lower panel illustrates UV absorbance profile at λ214 nm. Both *y* axes are in arbitrary units where the highest peak is default expressed as 100% of signal to illustrate component relative abundance. The retention times of NmS-17 and NmS-33 are indicated by arrows.

```
Toad   NmS-17                    DSSGIVGRPFFLFRPRNa
Toad   NmS-33          FLFQFSRAKDPSLKIGDSSGIVGRPFFLFRPRNa
Human  NmS-33          ILQRGSGTAAVDFTKKDHTATWGRPFFLFRPRNa
Mouse  NmS-36       LPRLLRLDSRMATVDFPKKDPTTSLGRPFFLFRPRNa
Rat    NmS-36       LPRLLHTDSRMATIDFPKKDPTTSLGRPFFLFRPRNa
                                  *     ***********

Frog   NmU-25       LKPDEELQGPGGVLSRGYFVFRPRNa
Frog   NmU-23         SDEEVQVPGGVISNGYFLFRPRNa
Human  NmU-25       FRVDEEFQSPFGSRSRGYFLFRPRNa
Rat    NmU-23       YKVNE-YQGP-GAPSGGFFLFRPRNa
Pig    NmU-25       FKVDEEFQGPIVSQNRRYFLFRPRNa
Dog    NmU-25       FRLDEEFQGPIASQVRRQFLFRPRNa
                       * *         * *****
```

Fig. 2. Comparative alignments of homologous amphibian and mammalian NmS and NmU sequences. * Denotes amino acid residue identities; *a* denotes C-terminal amide. Defining NmS motif is clearly a completely conserved C-terminal undecapeptide amide marked in bold italic contrasting with NmU whose defining motif is a completely conserved C-terminal pentapeptide amide marked in bold italic. Gaps have been inserted in the sequence of rat NmU-23 to maximize alignment.

peptides. The primary structures of toad NmS-17 and toad NmS-33 are compared with NmS peptides from human, mouse, and rat in Fig. 2. In addition, NmU peptides from amphibian and mammalian source tissues are included for comparison. The defining motif of NmS is evidently a fully conserved C-terminal undecapeptide amide that contrasts with the defining motif of NmU peptides, that is, a C-terminal pentapeptide amide. The C-terminal region of NmU has been established as the bioactive core of the molecule [1] and it is likely that this will also hold true for NmS peptides. However, NmS appears to have been more rigorously conserved in this region than its NmU relation during tetrapod evolution.

Cloning of NmS precursor cDNAs from venom-derived libraries

Using the strategy described in the Methods section, a single diffuse band was obtained following electrophoresis of 3′-RACE PCR products generated from each venom-derived library. Cloning of these PCR products revealed their heterogeneity as, following sequencing of over 200 clones, it was evident that six different transcript isoforms were present in *B. maxima* and in *B. orientalis* venom-derived libraries, but only a single transcript, corresponding to one of the *B. maxima/orientalis* isoforms, was present in the library from *B. variegata* venom. This may be of evolutionary significance as the first two species are of Asiatic origin whereas the latter is found in Central Europe. The longest open-reading frames encoded by the cloned cDNAs from each species are aligned in Fig. 3 and those of human, mouse, and rat are included as a sub-set for direct comparison. Figs. 4 and 5 show the aligned splice variant isoforms 1 through 6 obtained from *B. maxima* and *B. orientalis* venom-derived cDNA libraries, respectively. In common with the transcripts arising from the NmU gene in amphibians and mammals, the major region of splice variation occurs immediately upstream of the NmS-encoding domain. All

```
Human  MKHLRPQFPLILAIYCFCMLQIPSSGFPQPLADPSDGLDI
Mouse  MKHPLPHYSPILFIYCFCMLQIPSSGASPPLADSPDGLDI
Rat    MKHPFPQFPPILVIYCFCMLQIPSSGASPPLAGPPDGLDA
       ***  *    ** *************   ***   ****
BM     MRSEKHLLPLPLLLAICCLGTLHLSSGFPQSVPSYLEGLD
BO     MRSEKHLPPLPLLLAICCLGTLHPSSGFPQSVPSYMEALD
BV     MRSEKHLLPLPPLLAICCLGTLHLSSGFPQSVPSYLEGLD
       ******* *** *********** *********** * **

Human  VQLEQLAYCLSQWAPLSRQPKDNQDIYKRFLFHYSRTQEA
Mouse  VDPERLAYFLKQREIHSNQPKENQDVYKRFLFHYSRTRKP
Rat    VDPERLAHFLNQRETCSNQPKESRDVYKRFLFHYSRAWKS
       *  * **  * *    * ***   * **********
BM     IPESERHAFCFSQWTALQDQEQIPSFVMDLCSSIYNRMKV
BO     IPESEKLAFCFSQWTALPDQEQIPSFVMDLCSSIYNRMKV
BV     IPESE----------------IPSFVMDLCSSITNRMKV
       *****                ************ *****

Human  THPVKTGFPPVHPLMHLAAKLANRRMKRILQRGSGTAAVD
Mouse  THPVSAEFAPVHPLMRLAAKLASRRMKRLPRLLRLDSRMA
Rat    THPVNSEFAPVHPLMRLAAKLPSRRMKRLPRLLHTDSRMA
       ****   * ****** *****  *******
BM     NEENNHEIYKRFLFQFSRAKDPSLKIGESQIATAEYTKRD
BO     NEENNHEIYKRFLFQFSRTKDPSLKTGESQIATAEYTKRD
BV     NEENNHEIYKRFLFOFSRAKDPSLKIGESQIATAEYTKRD
       ****************** ****** **************

Human  ---FTKKDHTATWGRPFFLFRPRNGRNIEDEAQIQW
Mouse  TVDFPKKDPTTSLGRPFFLFRPRNGRYTDNNFQ---
Rat    TIDFPKKDPTTSLGRPFFLFRPRNGRYTDKV-Q---
          * *** *   *************       *
BM     SSGIVGRPFFLFRPRNGRKVSINEH
BO     SSGIVGRPFFLFRPRNGRKVSINEH
BV     SSGIVGRPFFLFRPRNGRKVSINEH
       *************************
```

Fig. 3. Alignment of full-length translated open-reading frames of NmS precursors from human, mouse, rat, and the toads, *B. maxima* (BM), *B. orientalis* (BO), and *B. variegata* (BV). * Denotes conserved residues in mammals; *denotes conserved residues in toads.

NmS cDNA isoforms from the bombinid toads studied here have been deposited in the EMBL Nucleotide Sequence Database under the Accession Nos. AM115659 through AM115671.

Pharmacological investigation of stable NmU receptor-transfected CHO cell lines

Synthetic replicates of toad NmS-17 and toad NmS-33 were investigated for activity using CHO cell lines (CHO/FM-3-14 and CHO/FM-4-16) that had been stably transfected with either human FM-3/GPR66 or FM-4/TGR-1 NmU/NmS receptors. Human and rat NmS were tested at the same time in all experiments as internal controls for comparative purposes. The dose–response curves for each peptide ligand and at each NmU receptor-transfected CHO cell line are shown in Fig. 6. All NmS peptides tested generated classical sigmoidal dose–response curves, as assessed by quantitative changes in fluorescence intensity within the concentration range (10^{-13} M through 10^{-7} M) employed, and were of a high and comparable order of potency effecting receptor activation in the sub-nanomolar range. The calculated EC_{50} values for each NmS peptide at each receptor are summarized in Table 1 for clarification of